Super-resolution in fluorescence microscopy by fluctuations of molecules and curve modeling

Laure Blanc-Féraud

Equipe Morpheme, (CNRS, UCA, INRIA SAM),
Laboratoire I3S, Sophia Antipolis.

AI WILD WEST Workshop, 29-30 January 2026

1. Fluorescence microscopy, limited resolution
   Inverse problem
   $$\mathcal{F}(x, data) + \mathcal{R}(x)$$
2. Data-driven method: FluoGAN
   $$\mathcal{F}(x, data) + \mathcal{R}(x)$$
3. Off-the-grid method promoting curves
   $$\mathcal{F}(x, data) + \mathcal{R}(x)$$

Curves in fluorescent microscopy

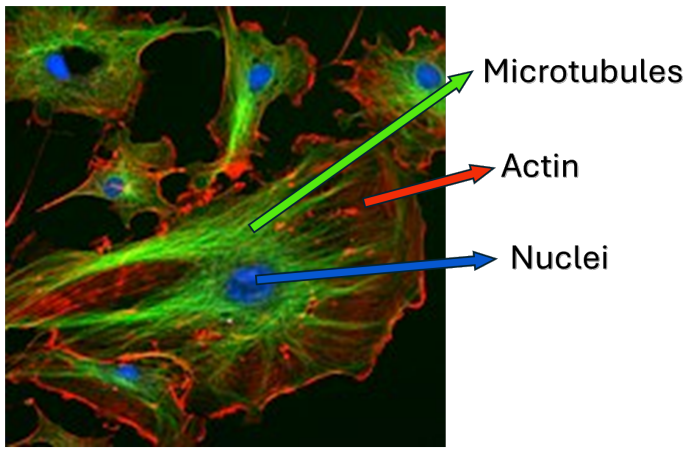

- Fluorescent cell

Curves in fluorescent microscopy

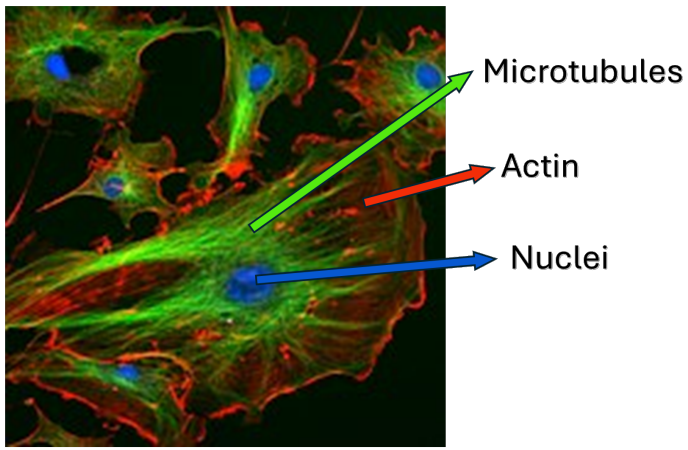

✤ Fluorescent cell

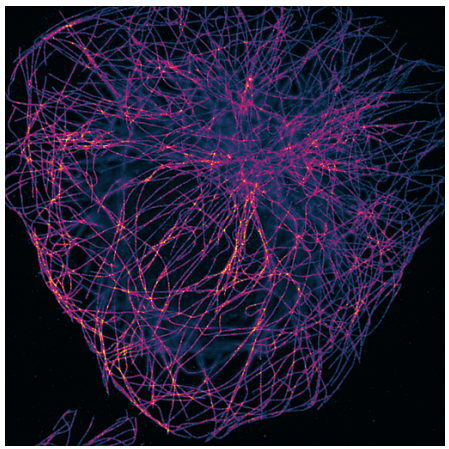

✤ Image of microtubules

Curves in fluorescent microscopy

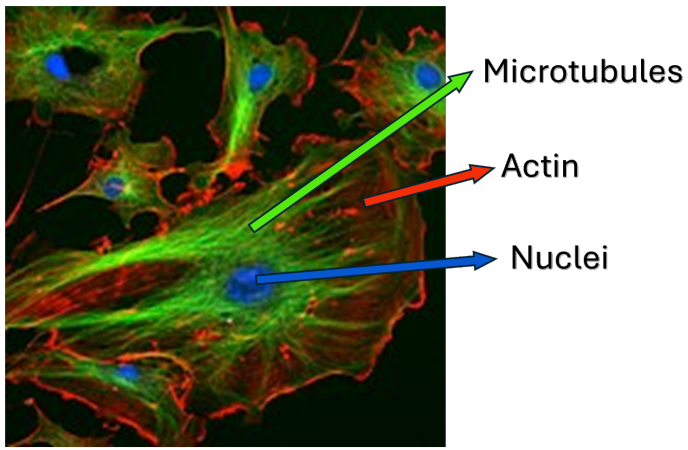

✤ Fluorescent cell

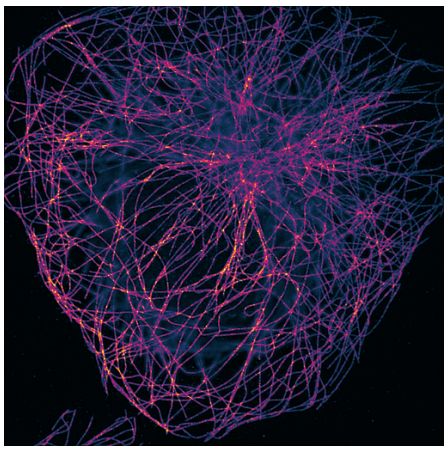

✤ Image of microtubules

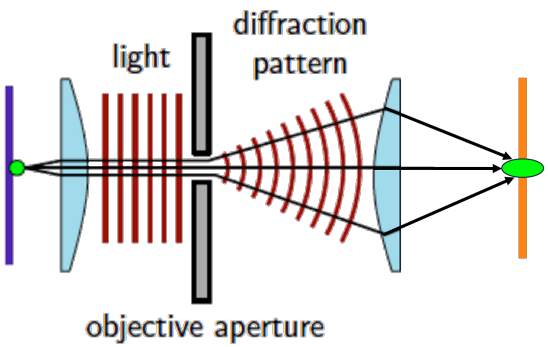

✤ Diffraction limit

Curves in fluorescent microscopy

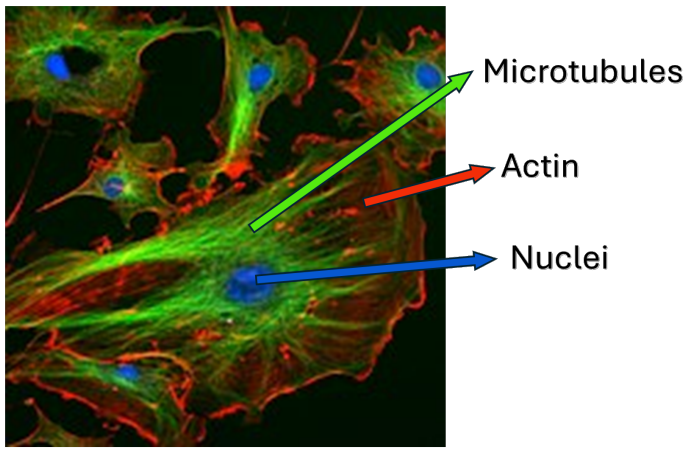

✤ Fluorescent cell

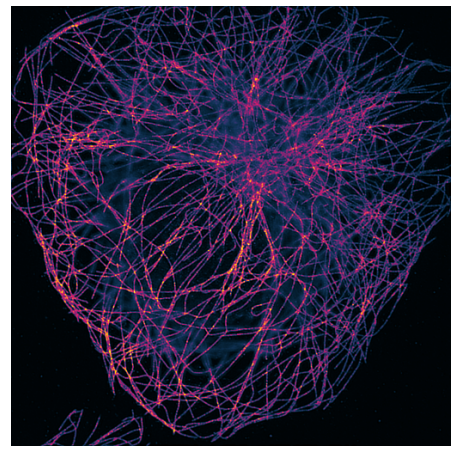

✤ Image of microtubules

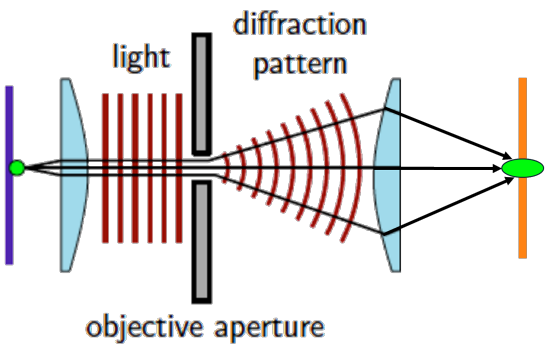

✤ Diffraction limit

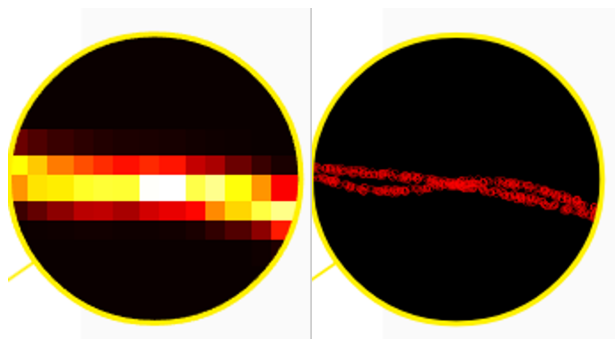

✤ Blurred curves

State-of-the-art methods for SR microscopy

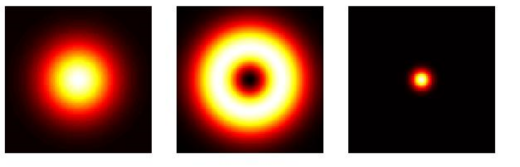

Wikipedia

STimulation-Emission-Depletion ([Hell, Wichmann, '94])

- Depletes some of the excited fluorescent molecules, limiting the area of illumination
- Special equipment required, potentially harmful excitation levels

Single **M**olecule **L**ocalization **M**icroscopy ([Betzig, Zhuang, Hess, '06])

- Only few molecules activated for better localisation
- Time consuming acquisition, poor temporal resolution, potentially harmful excitation levels

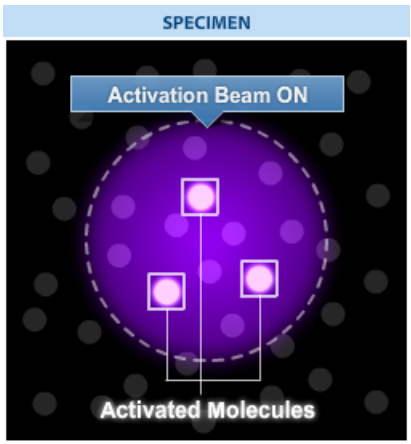

http://zeiss-campus.magnet.fsu.edu/

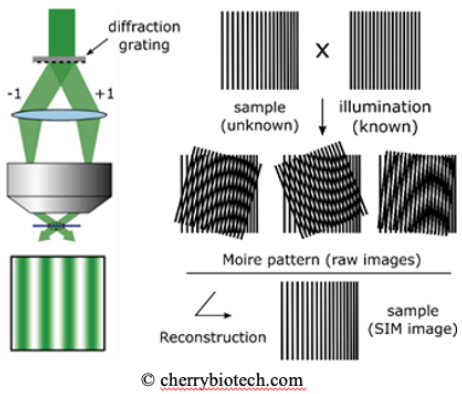

Structured **I**llumination **M**icroscopy ([Gustafsson, M. G. et al. '08])

- Special illumination required, limited super-resolution power

State-of-the-art methods for SR microscopy

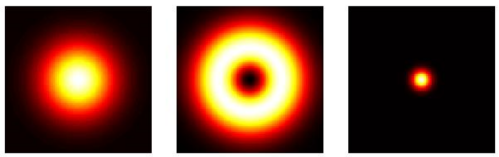

Wikipedia

STimulation-Emission-Depletion ([Hell, Wichmann, '94])

- Depletes some of the excited fluorescent molecules, limiting the area of illumination
- Special equipment required, potentially harmful excitation levels

Single Molecule Localization Microscopy ([Betzig, Zhuang, Hess, '06])

- Only few molecules activated for better localisation
- Time consuming acquisition, poor temporal resolution, potentially harmful excitation levels

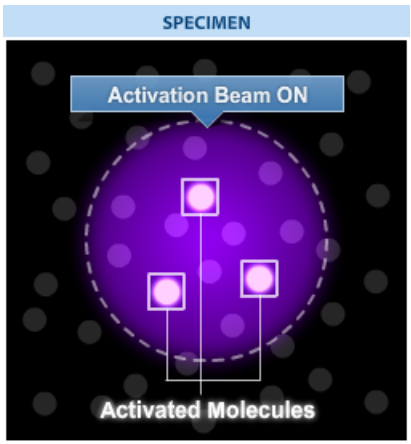

http://zeiss-campus.magnet.fsu.edu/

Objective

Design an SR model with the following features:

- dealing with high density samples
- method non harmful for the biological sample
- **use of standard equipment/conventional fluorophores**

Super-Resolution: Fluctuation-based Methods

Main Idea

Exploiting the stochastic temporal fluctuations of individual fluorophores.

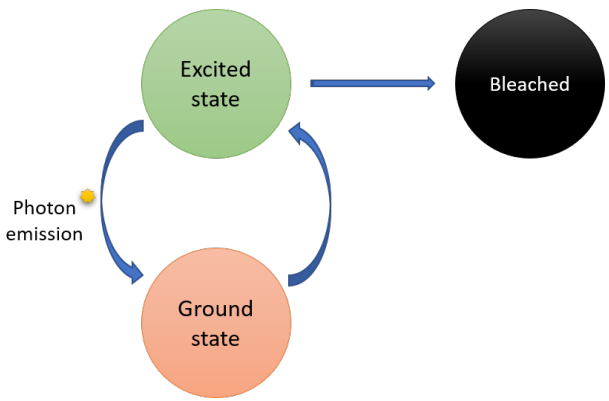

Fluorophore states

Super-Resolution: Fluctuation-based Methods

Main Idea

Exploiting the stochastic temporal fluctuations of individual fluorophores.

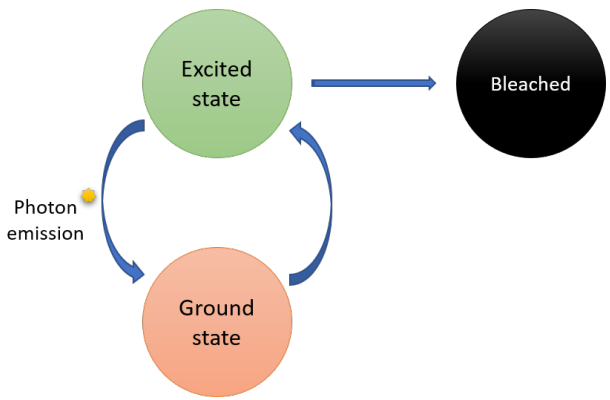

Fluorophore states

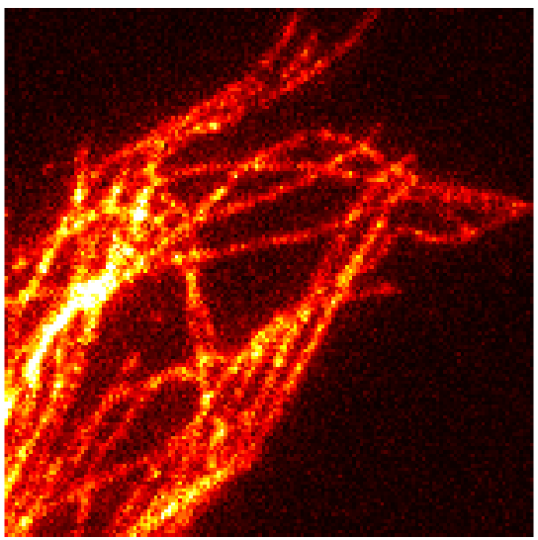

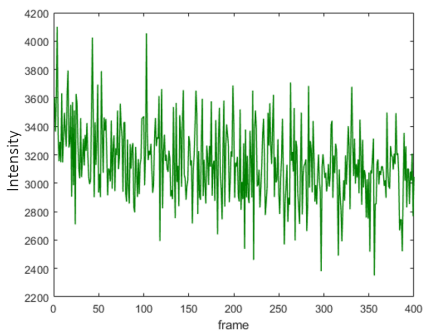

Temporal profile of a pixel

SOFI [Dertinger et al.'09]; SRRF [Gustafsson et al.'16], SPARCOM [Solomon et al.'19], COLORME [Stergiopoulou et al.'22]

Mathematical Modeling

$\mathbf{Y_t} \in \mathbb{R}^{M \times M}$ $\quad$ $\mathbf{X_t} \in \mathbb{R}^{L \times L}$

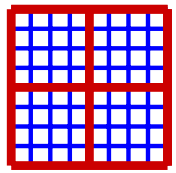

$q \in \mathbb{N}$

$L = qM$

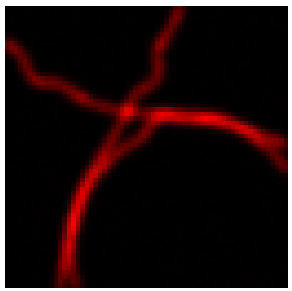

$= \mathcal{P}\Big($ $\mathbf{\Psi}$

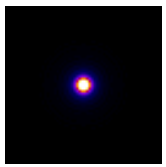

$*$

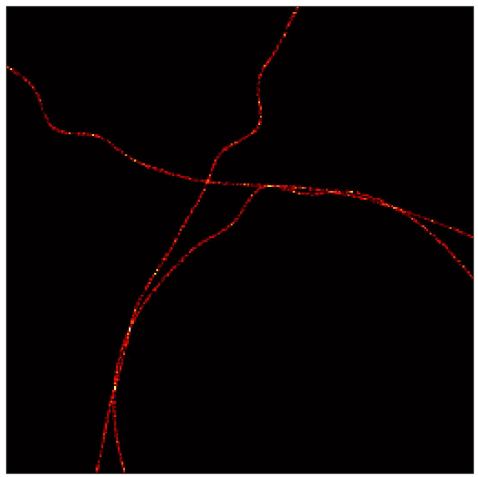

$+\mathbf{B}\Big) + \mathbf{N_t}$

$$\mathbf{y_t} = \mathcal{P}(\mathbf{\Psi x_t} + \mathbf{b}) + \mathbf{n_t}\,, \quad \forall t = 1, \ldots, T$$

- $\mathbf{y_t} \in \mathbb{R}^{M^2}$: LR acquisitions
- $\mathbf{x} := \frac{1}{T}\sum_{t=1}^{T} \mathbf{x_t} \in \mathbb{R}^{L^2}$: HR image ($L = qM$)
- $\mathbf{\Psi} \in \mathbb{R}^{M^2 \times L^2}$: forward operator, PSF convolution (diffraction and sampling)
- $\mathbf{n_t} \in \mathbb{R}^{M^2}$: additive white Gaussian noise, $\mathbf{n_t} \sim \mathcal{N}(\mathbf{0}, s\mathbf{I})$
- $\mathbf{b} \in \mathbb{R}^{M^2}$: temporally-constant background
- $\mathcal{P}(\tau)$: Poisson random variable of parameter τ

Super-Resolution: Fluctuation-based Methods

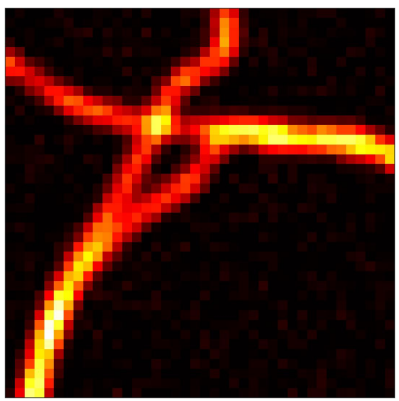

(a) $\mathbf{y_t}$, Low Background, SNR $\approx$ 15.6 dB.Video rate: 100 fps.

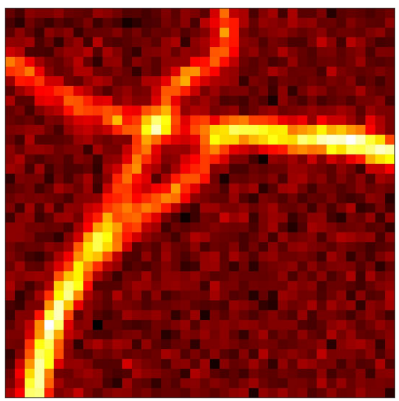

(b) $\mathbf{y_t}$. High background, very low SNR. Video rate: 100 fps.

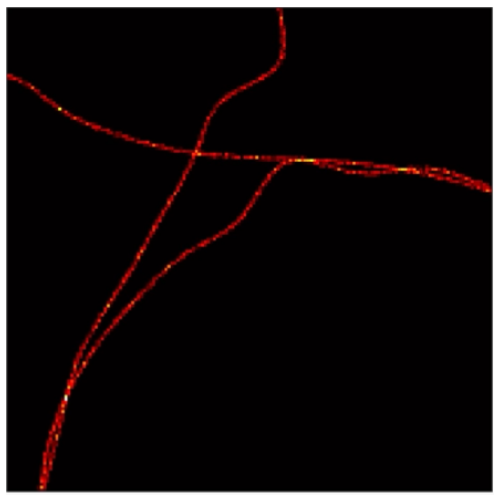

(c) Mean of the molecule fluctuations

Data-driven and model-based methods in inverse problems

- **Neural Network revolution → Application to inverse problems**
- For **inverse problems**, we want to keep the physical knowledge of the acquisition system
- Plug and Play (PnP) [Kamilov'18,Pesquet'21...]
- Bi-level [Calatroni'16,Holler'18,Gunter'22...]
- Unrolling algorithms [Fessler'20, Monga'20...]
- Generative networks VAE [Goh'19, Gonzales'19...], GAN [Shah'18,Gupta'21...], Flow Matching [Martin'25, Meanti'25, Peyre'25...]

1. Fluorescence microscopy, limited resolution
   Inverse problem
   $$\mathcal{F}(x, data) + \mathcal{R}(x)$$

2. Data-driven method: FluoGAN
   $$\mathcal{F}(x, data) + \mathcal{R}(x)$$

3. Off-the-grid method promoting curves
   $$\mathcal{F}(x, data) + \mathcal{R}(x)$$

Idea of the method

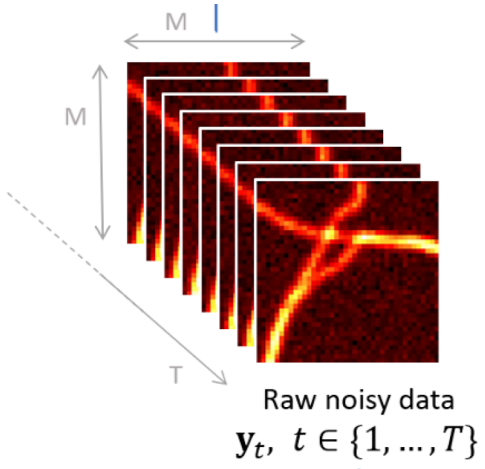

- Use all the diversity of the data: use the frames of the video $\mathbf{y}_t^{\text{real}}$ as samples of the observed distribution $\mathcal{D}^{real}$
  - not only a summary as the mean $\overline{\mathbf{y}}$, or the covariance matrix $\mathbf{r}_{\mathbf{y}}$,

Idea of the method

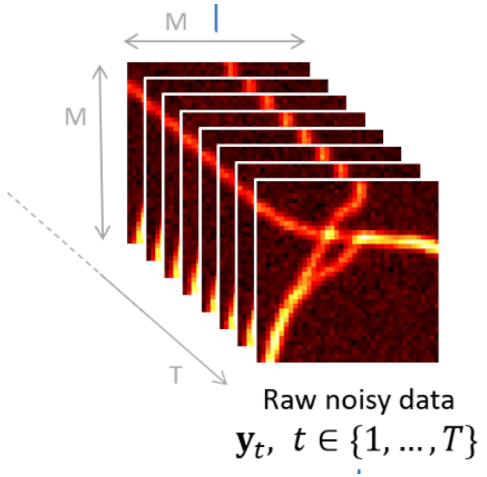

- Use all the diversity of the data: use the frames of the video $\mathbf{y}_t^{\text{real}}$ as samples of the observed distribution $\mathcal{D}^{real}$
  - not only a summary as the mean $\overline{\mathbf{y}}$, or the covariance matrix $\mathbf{r}_{\mathbf{y}}$,
- $\mathbf{x}, \mathbf{b}$ through the physical model of acquisition follows the simulated distribution $\mathbf{y}_t^{\text{sim}} \sim \mathcal{D}^{\text{sim}}(\mathbf{x}, \mathbf{b}) \approx \alpha \mathcal{P}\left(\mathbf{\Psi x} + \mathbf{b}\right) + \mathbf{n}$

given $\left\{\mathbf{y}_t^{\text{real}}\right\}_{t=1}^{T}$ find $(\mathbf{x}, \mathbf{b}) \in \mathbb{R}^{L^2} \times \mathbb{R}^{M^2}$ s.t. $\mathcal{D}^{\text{sim}}(\mathbf{x}, \mathbf{b}) \sim \mathcal{D}^{\text{real}}$

$$\text{given } \left\{\mathbf{y}_t^{\text{real}}\right\}_{t=1}^{T} \quad \text{find } (\mathbf{x},\mathbf{b}) \in \mathbb{R}^{L^2} \times \mathbb{R}^{M^2} \quad \text{s.t.}$$

$$\min_{\mathbf{x}\in\mathbb{R}_+^{L^2},\ \mathbf{b}\in\mathbb{R}_+^{M^2}} d(\mathcal{D}^{\text{sim}}(\mathbf{x},\mathbf{b}),\mathcal{D}^{\text{real}}) + \mathcal{R}_1(\mathbf{x}) + \mathcal{R}_2(\mathbf{b}),$$

$$\mathcal{D}^{\text{sim}}(\mathbf{x},\mathbf{b}) \approx \alpha\mathcal{P}\left(\mathbf{\Psi}\mathbf{x}+\mathbf{b}\right)+\mathbf{n}$$

We use the **Wasserstein distance** between the probabilities, computed through the Wasserstein GAN network [Arjovsky *et al.*'17] ,

Generative Adversarial Networks (GANs)

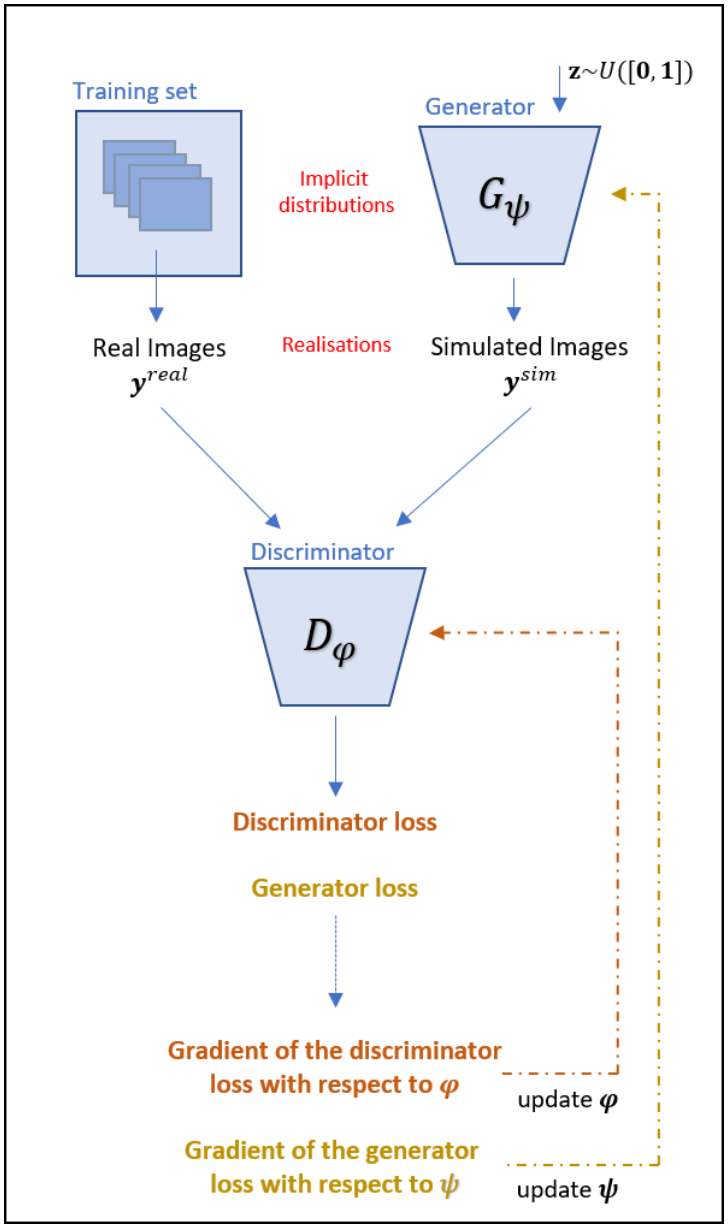

Generative Adversarial Networks (GANs)

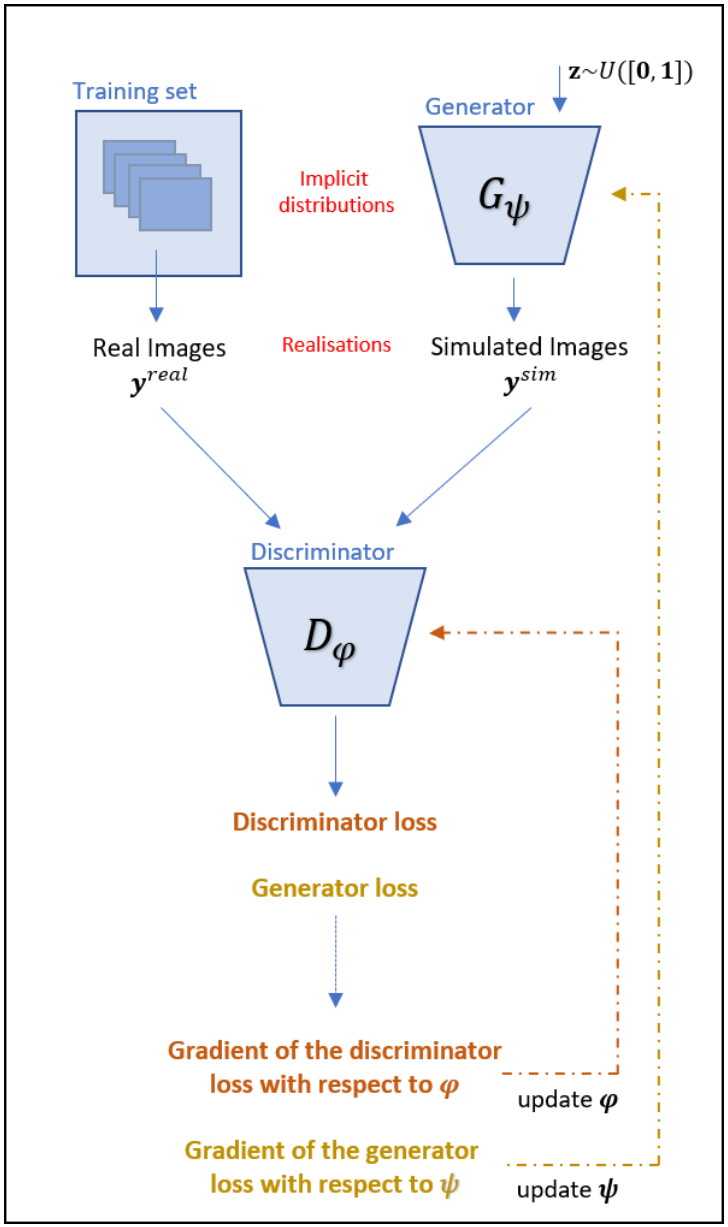

Minimax game [Goodfellow et al., '14]

$$\min_{\psi} \max_{\varphi} \; \mathbb{E}_{\mathbf{y}^{\text{real}}} \left(D_\varphi(\mathbf{y}) \right) - \mathbb{E}_{\mathbf{y}^{\text{sim}}} \left(D_\varphi(\mathbf{y}^{\text{sim}}(\psi)) \right)$$

Generative Adversarial Networks (GANs)

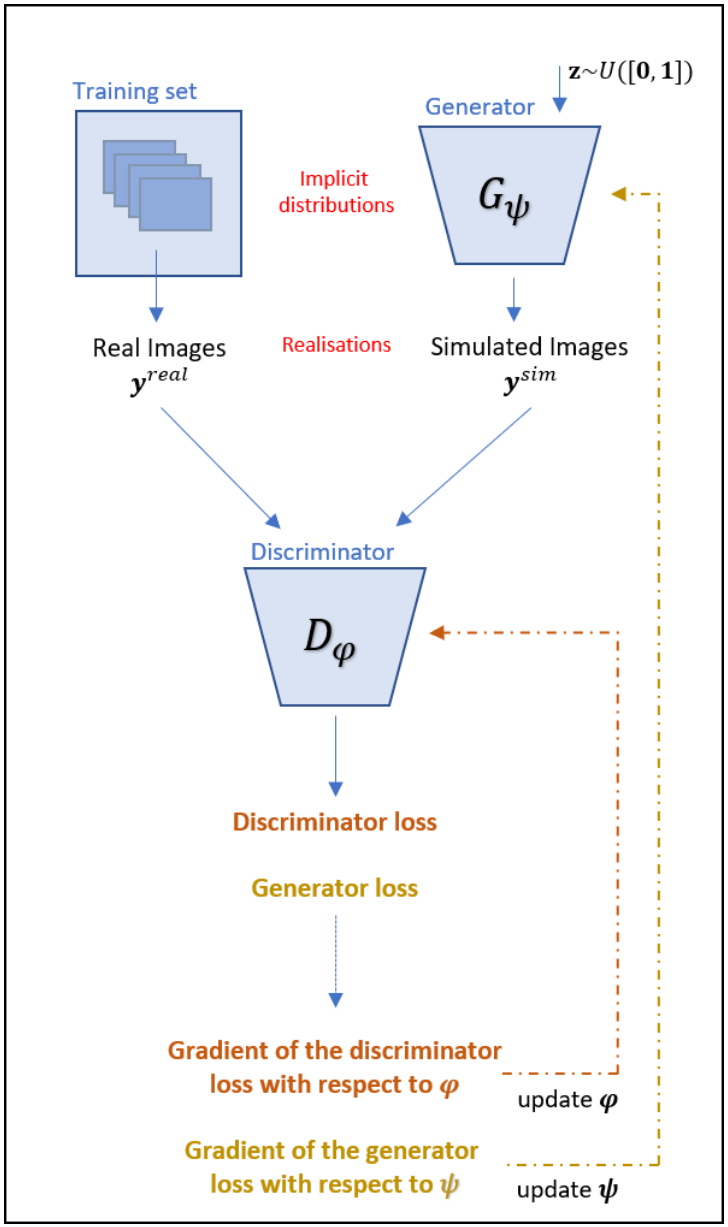

Minimax game [Goodfellow et al., '14]

Wasserstein GAN [Gulrajani,Ahmed, Arjovsky, Dumoulin, Courville'17]

$$\min_{\psi}\max_{\varphi}\ \mathbb{E}_{\mathbf{y}^{\text{real}}}\left(D_\varphi(\mathbf{y})\right)-\mathbb{E}_{\mathbf{y}^{\text{sim}}}\left(D_\varphi(\mathbf{y}^{\text{sim}}(\psi))\right)$$
$$-\lambda\mathbb{E}_{\mathbf{y}^{\text{mix}}}\left(\left(\|\nabla_{\mathbf{y}}D_\varphi(\mathbf{y}^{\text{mix}})\|-1\right)^2\right)$$

where

$$\mathbf{y}^{\text{mix}}:=\eta\mathbf{y}^{\text{sim}}(\psi)+(1-\eta)\mathbf{y}^{\text{real}},\quad \eta\sim\mathcal{U}([0,1])$$

- distributions with non overlapping support
- avoid vanishing gradient

Generative Adversarial Networks (GANs)

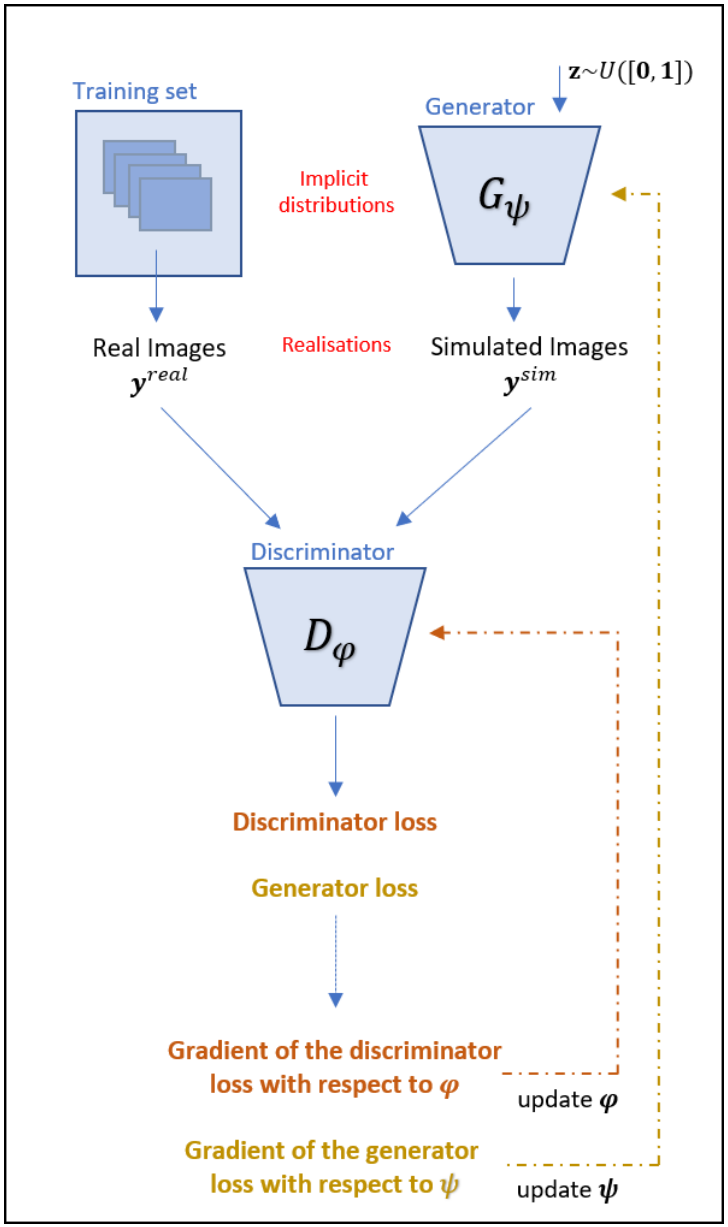

FluoGAN inspired from [Gupta, McCann, Donati,Unser,'21]

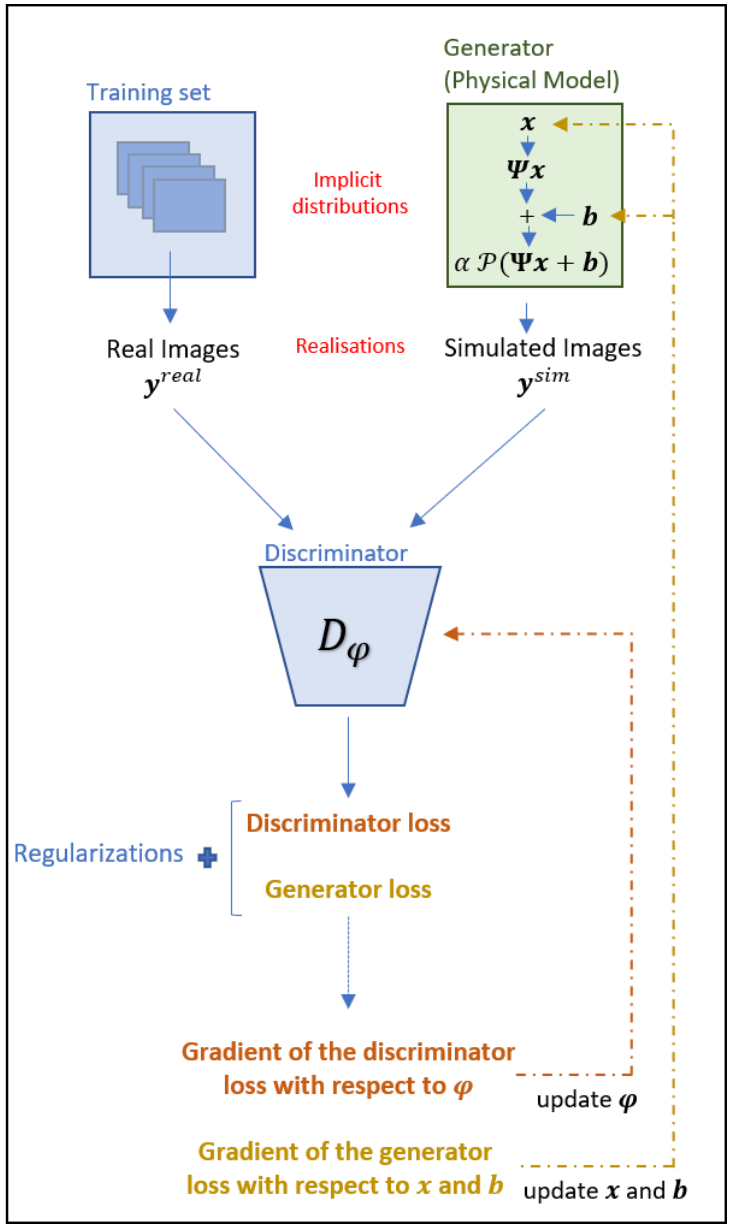

Losses and regularization

$$\text{Discr.: } \min_{\varphi} \left\{ \sum_{m=1}^{M} D_\varphi(\mathbf{y}_m^{\text{sim}}(\mathbf{x},\mathbf{b})) - \sum_{m=1}^{M} D_\varphi(\mathbf{y}_m^{\text{real}}) + \lambda_D \sum_{m=1}^{M} \left(\|\nabla_y D_\varphi(\mathbf{y}_m^{\text{mix}}(\mathbf{x},\mathbf{b}))\| - 1 \right)^2 \right.$$

$$\text{Gen.: } \min_{\mathbf{x},\mathbf{b}} \left\{ - \sum_{m=1}^{M} D_\varphi(\mathbf{y}_m^{\text{sim}}(\mathbf{x},\mathbf{b})) + \gamma \sum_{m=1}^{M} \|\mathbf{y}_m^{\text{sim}}(\mathbf{x},\mathbf{b}) - \bar{\mathbf{y}}^{\text{real}}\|^2 \right.$$

$$\left. + \lambda_1 \|\mathbf{x}\|_1 + \lambda_2 \|\nabla \mathbf{b}\|_2^2 + \iota_{\geq 0}(\mathbf{x}) + + \iota_{\geq 0}(\mathbf{b}) \right\},$$

$$\gamma, \lambda_1, \lambda_2 \geq 0, \ \lambda_D > 0$$

- $y_m^{\text{sim}}(\mathbf{x},\mathbf{b})$ generated via the physical model $\mathbf{y}_m^{\text{sim}} \sim \mathcal{D}^{\text{sim}}(\mathbf{x},\mathbf{b}) \approx \alpha \mathcal{P}(\mathbf{\Psi x} + \mathbf{b}) + \mathbf{n}$
- WGAN with gradient penalisation to avoid vanishing gradients
- ℓ_2-fidelity to favour convergence (at least in the earlier epochs)
- (optional) *a-priori* solution requirements

Geometrical Argolight calibrated sample

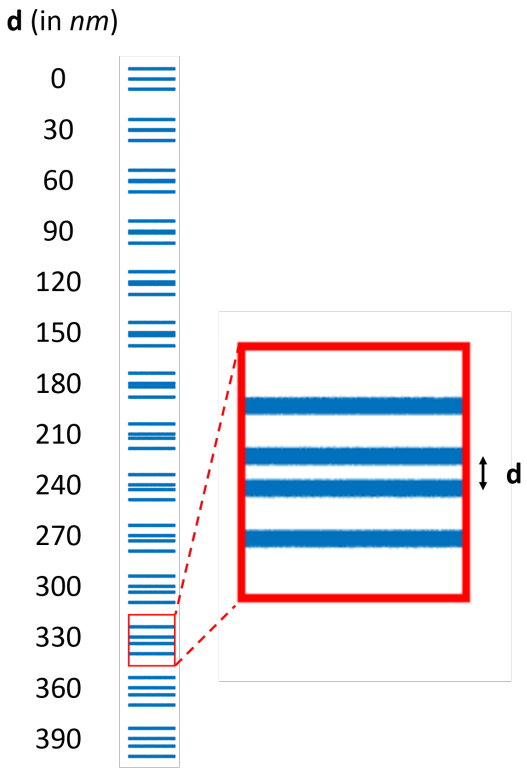

Spatial structure of simulated/real calibrated sample (ARGO-CR slide, Argolight)

- Real Data (epifluorescence microscope):
  Pixel size = 103 nm, FWHM = 270 nm, Acquired images = 500 @ 10 fps.

Real Data: ARGO-CR calibrated slide

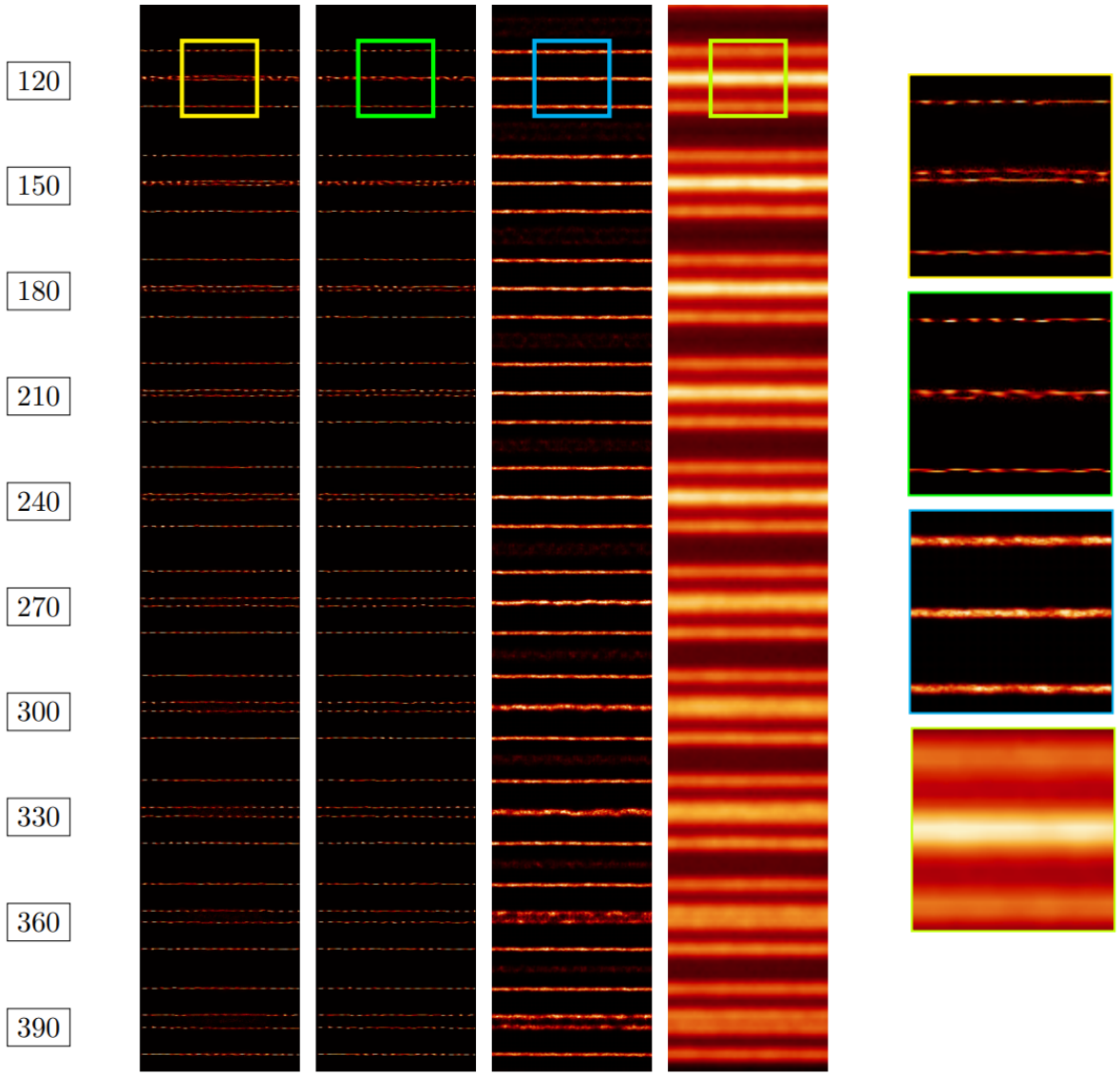

(a) FluoGAN (with D_φ) (b) FluoGAN (w.o. D_φ) (c) SRRF (d) $\bar{y}$

Real Data: Osteopsis Ovata

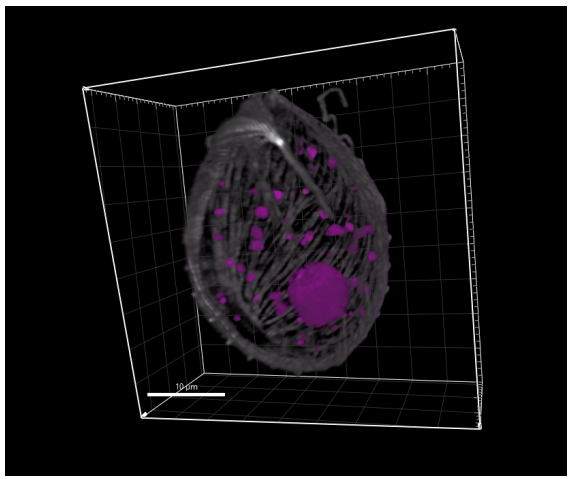

(a) Confocal 3D image of *Ostreopsis Ovata* with microtubules (white) and DNA (magenta).

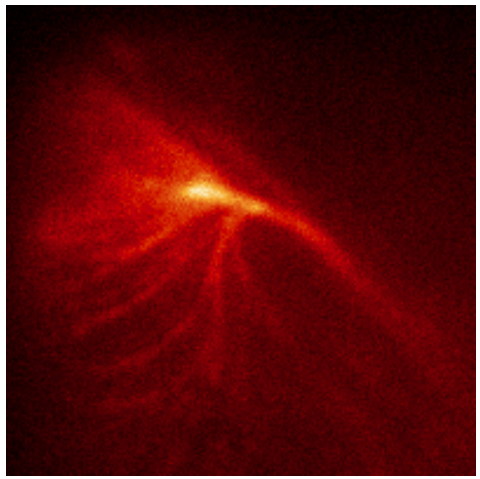

(b) Low-resolution epifluorescent image (sample average) of the microtubules tip.

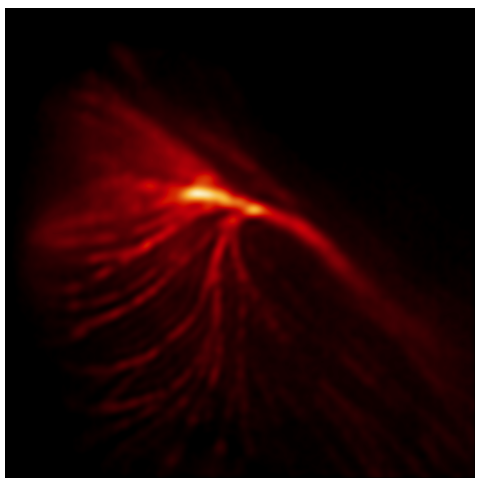

(c) FluoGAN reconstruction of Fig. 4b.

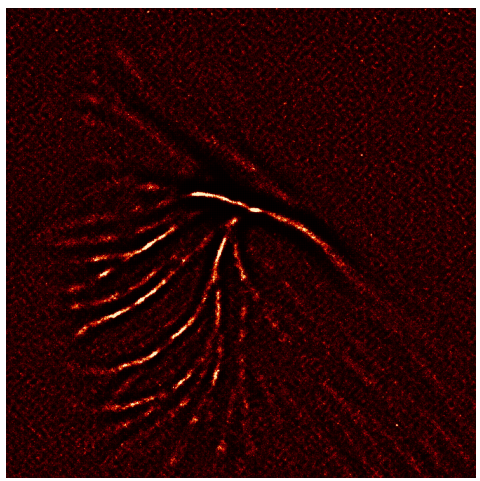

(d) SRRF reconstruction of Fig. 4b.

M. Cachia, V. Stergiopoulou, L. Calatroni, S. Schaub, L. Blanc-Féraud. "Fluorescence image deconvolution microscopy via generative adversarial learning (FluoGAN)," [Inverse Problems, 2023].

Code available at `https://github.com/cmayeul/FluoGAN`

Continuing

- Use of a more accurate model
  (e.g. $p^{\mathrm{sim}}(\mathbf{x}, \mathbf{b}) := \alpha \mathcal{P}\left(\mathbf{\Psi} \mathcal{P}(\mathbf{x}) + \mathbf{b}\right) + \mathbf{n}$)
- Use flow matching to minimize KL distance [Meanti'25]
- PSF, parameter estimation,
- Validation: quantitative criteria, more data, statistical studies.

1. Fluorescence microscopy, limited resolution
   Inverse problem
   $$\mathcal{F}(x, data) + \mathcal{R}(x)$$
2. Data-driven method: FluoGAN
   $$\mathcal{F}(x, data) + \mathcal{R}(x)$$
3. Off-the-grid method promoting curves
   $$\mathcal{F}(x, data) + \mathcal{R}(x)$$

Grid or gridless?

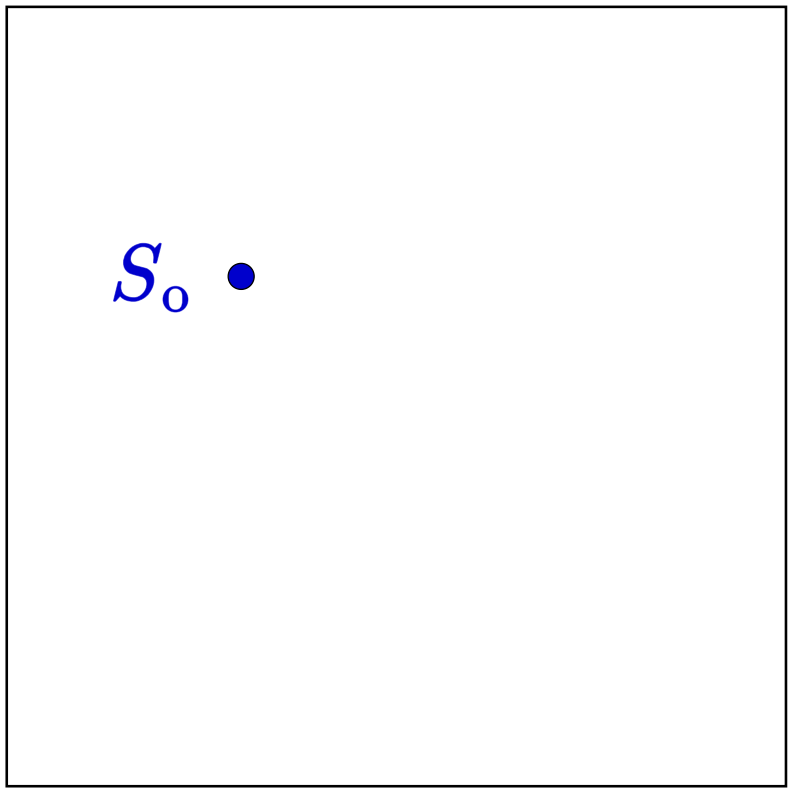

Source to estimate

Grid or gridless?

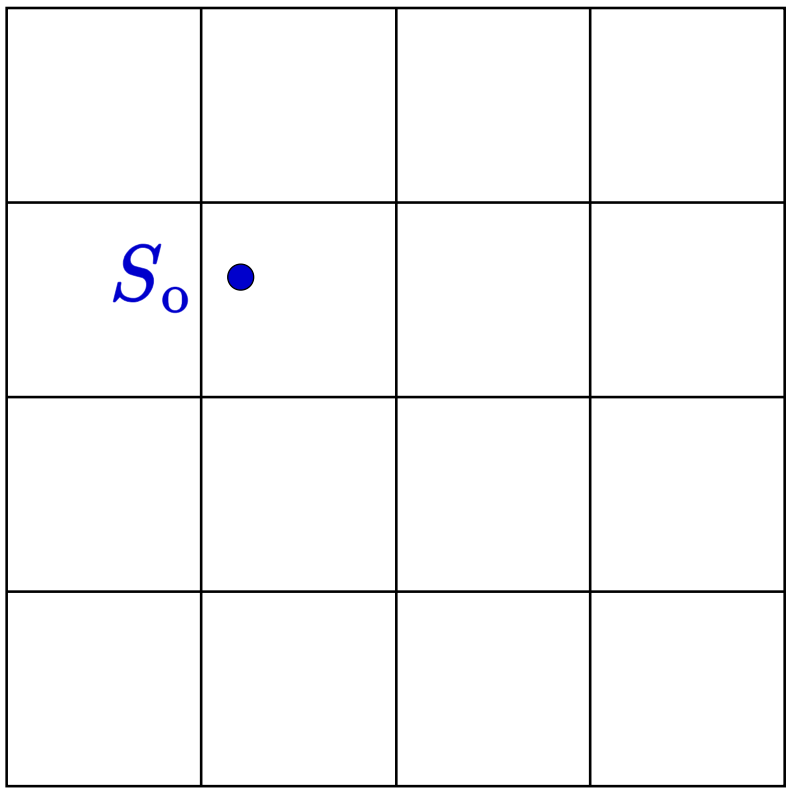

Introducing a grid

Grid or gridless?

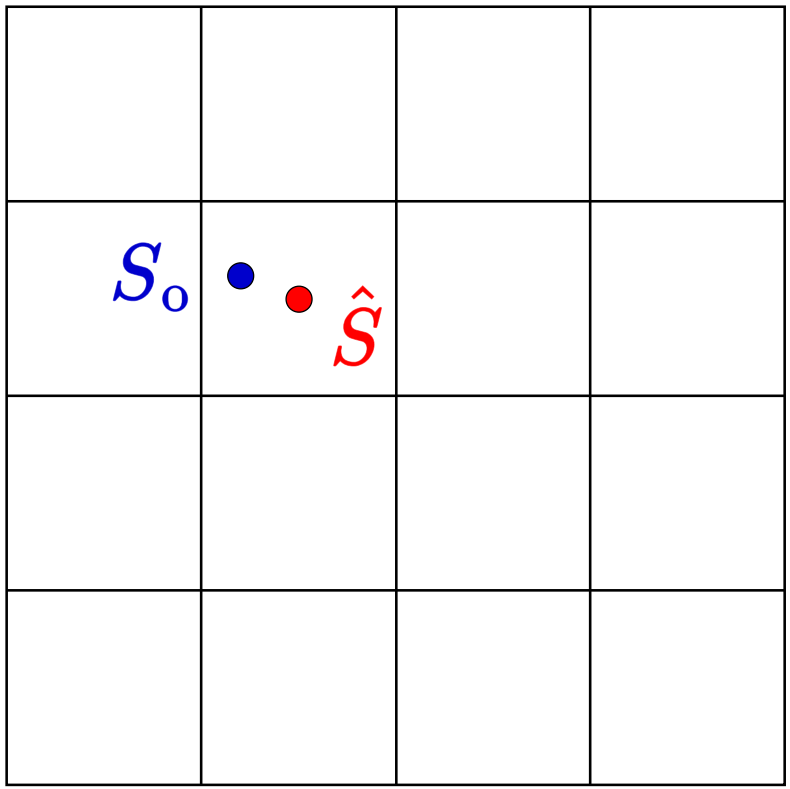

Reconstruction $\hat{S}$ on a grid

Grid or gridless?

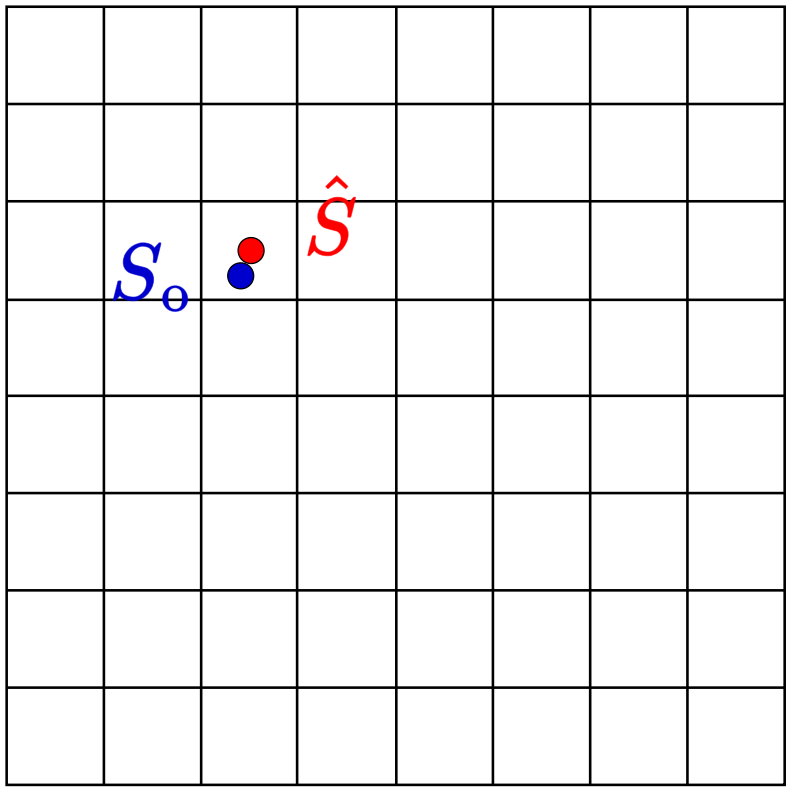

Reconstruction $\hat{S}$ on a finer grid

Grid or gridless?

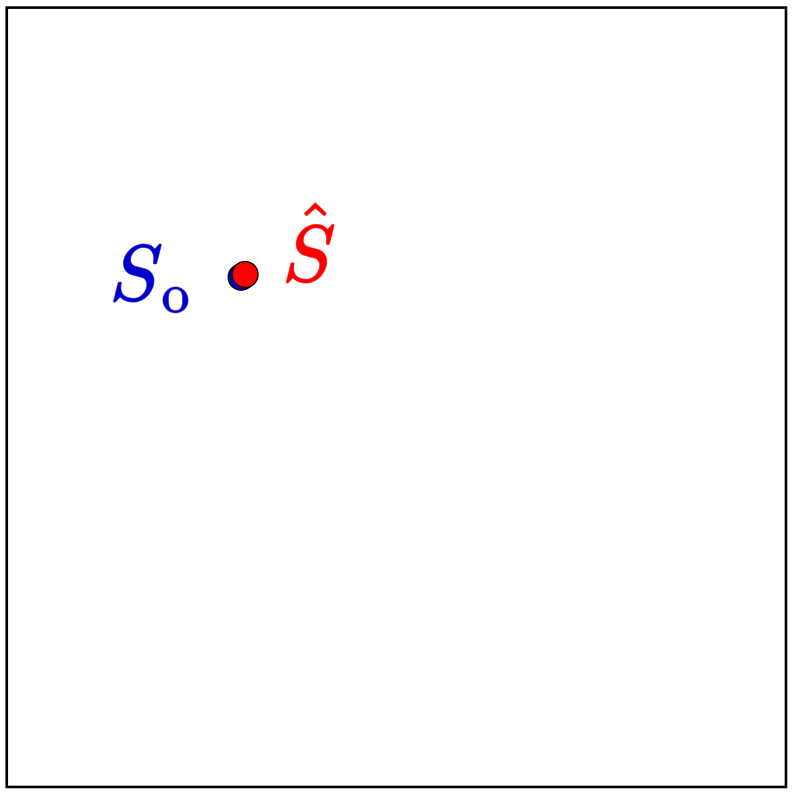

Reconstruction $\hat{S}$ is now **off-the-grid**

For spikes : sparse signals

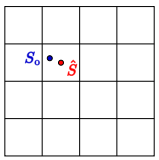

Discrete case

- the reconstructed peaks are necessarily on the fine grid;
- (Non-)convex combinatorial optimisation;
- fast numerical computation;
- large literature.

$$\underset{\mathbf{u}\in\mathbb{R}^N}{\arg\min}\ \frac{1}{2}\|\mathbf{y}-\Psi\mathbf{u}\|_2^2+\lambda\|\mathbf{u}\|_{0 \text{ or } 1}$$

For spikes : sparse signals

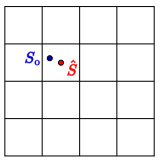

Discrete case

- the reconstructed peaks are necessarily on the fine grid;
- (Non-)convex combinatorial optimisation;
- fast numerical computation;
- large literature.

$$\underset{\mathbf{u}\in\mathbb{R}^N}{\arg\min}\ \frac{1}{2}\|\mathbf{y}-\Psi\mathbf{u}\|_2^2+\lambda\|\mathbf{u}\|_{0 \text{ or } 1}$$

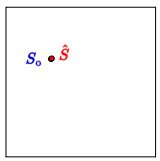

Off-the-grid case

- not limited by the grid;
- convexity of the functional on an infinite dimensional space;
- existence and uniqueness guarantees;
- more recent field of research.

$$\underset{m\in\mathcal{M}(\mathcal{X})}{\arg\min}\ \frac{1}{2}\|\mathbf{y}-\Psi m\|_2^2+\lambda\|m\|_{\mathsf{TV}}$$

Reconstruction of points

BLASSO functional: [De Castro Gamboa 2012, Duval Peyré 2014]

$$\underset{m \in \mathcal{M}(\mathcal{X})}{\arg\min} \frac{1}{2} \|\mathbf{y} - \Psi m\|_2^2 + \lambda \|m\|_{\mathsf{TV}}$$

- $\mathbf{y} \in \mathbb{R}^N$: observed image (blurred + additive Gaussian noise)
- $\Psi : \mathcal{M}(\mathcal{X}) \to \mathbb{R}^N$ linear map

Reconstruction of points

BLASSO functional: [De Castro Gamboa 2012, Duval Peyré 2014]

$$\underset{m \in \mathcal{M}(\mathcal{X})}{\arg\min} \frac{1}{2} \|\mathbf{y} - \Psi m\|_2^2 + \lambda \|m\|_{\mathsf{TV}}$$

- $\mathbf{y} \in \mathbb{R}^N$: observed image (blurred + additive Gaussian noise)
- $\Psi : \mathcal{M}(\mathcal{X}) \to \mathbb{R}^N$ linear map

- $\mathcal{M}(\mathcal{X}) = \mathcal{C}_0(\mathcal{X}, \mathbb{R})^*$
- $\|m\|_{\mathsf{TV}} = \sup \left\{ \langle m, \varphi \rangle \,,\ \varphi \in \mathcal{C}_0(\mathcal{X}, \mathbb{R}),\ \|\varphi\|_{\infty, \mathcal{X}} \leq 1 \right\}$

Off-the-grid reconstruction of points

BLASSO functional: [De Castro Gamboa 2012, Duval Peyré 2014]

$$\underset{m \in \mathcal{M}(\mathcal{X})}{\arg\min} \underbrace{\frac{1}{2} \|\mathbf{y} - \Psi(m)\|_2^2}_{\text{data fidelity term}} + \underbrace{\lambda \|m\|_{\mathsf{TV}}}_{\text{regularization}}$$

$$m^* = \sum_{i=1}^{r} a_i \delta_{x_i}$$

- Result from the **representer theorem** [Boyer et al. 2019; Bredies &Carioni 2020] : one of the minimizers is a finite sum of Diracs $(r \leq N)$.

Off-the-grid reconstruction of points

BLASSO functional: [De Castro Gamboa 2012, Duval Peyré 2014]

$$\underset{m \in \mathcal{M}(\mathcal{X})}{\arg\min} \underbrace{\frac{1}{2} \|\mathbf{y} - \Psi(m)\|_2^2}_{\text{data fidelity term}} + \underbrace{\lambda \|m\|_{\mathsf{TV}}}_{\text{regularization}}$$

$$m^* = \sum_{i=1}^{r} a_i \delta_{x_i}$$

- Result from the **representer theorem** [Boyer et al. 2019; Bredies &Carioni 2020] : one of the minimizers is a finite sum of Diracs ($r \leq N$).
- Difficult numerical problem: infinite dimensional, non reflexive space of optimization, no Hilbertian structure: no proximal algorithm,

Off-the-grid reconstruction of points

BLASSO functional: [De Castro Gamboa 2012, Duval Peyré 2014]

$$\underset{m \in \mathcal{M}(\mathcal{X})}{\arg\min} \underbrace{\frac{1}{2} \|\mathbf{y} - \Psi(m)\|_2^2}_{\text{data fidelity term}} + \underbrace{\lambda \|m\|_{\mathsf{TV}}}_{\text{regularization}}$$

$$m^* = \sum_{i=1}^{r} a_i \delta_{x_i}$$

- Result from the **representer theorem** [Boyer et al. 2019; Bredies &Carioni 2020] : one of the minimizers is a finite sum of Diracs ($r \leq N$).
- Difficult numerical problem: infinite dimensional, non reflexive space of optimization, no Hilbertian structure: no proximal algorithm,
- Tackled by greedy algorithm as (Sliding) Franck-Wolf (conditional gradient descent algorithm) [Denoyelle et al. 2019].

Representer theorem for TV norm

$$\underset{m \in \mathcal{M}(\mathcal{X})}{\arg\min} \frac{1}{2}\|\mathbf{y} - \Psi m\|_2^2 + \lambda \|m\|_{\mathsf{TV}} \quad \leftarrow \quad \text{Point reconstruction}$$

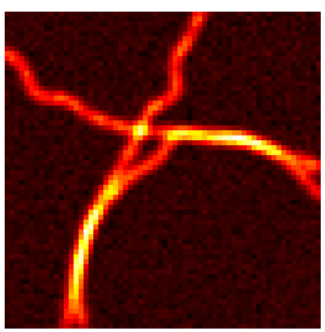

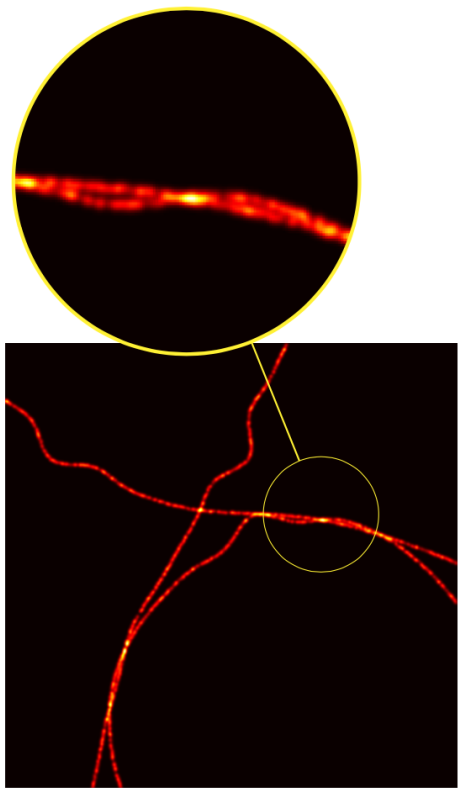

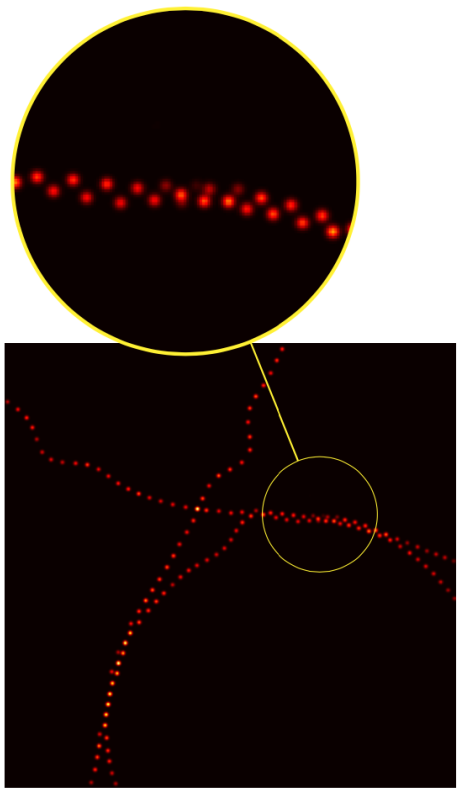

Curve reconstruction with CROC energy

CROC functional: [Laville, Blanc-Féraud, Aubert 2023]

$$\arg\min_{\mathbf{m}\in\mathcal{V}} \frac{1}{2}\|\mathbf{y}-\Psi\mathbf{m}\|_2^2 + \alpha(\|\mathbf{m}\|_{\mathsf{TV}^2} + \|\operatorname{div}\mathbf{m}\|_{\mathsf{TV}})$$

$$\mathbf{m}^* = \sum_{i=1}^{r} a_i \mu_{\gamma_i}$$

Curve reconstruction with CROC energy

CROC functional: [Laville, Blanc-Féraud, Aubert 2023]

$$\arg\min_{\mathbf{m}\in\mathscr{V}} \frac{1}{2}\|\mathbf{y}-\Psi\mathbf{m}\|_2^2 + \alpha(\|\mathbf{m}\|_{\mathsf{TV}^2} + \|\operatorname{div}\mathbf{m}\|_{\mathsf{TV}})$$

$$\mathbf{m}^* = \sum_{i=1}^{r} a_i \mu_{\gamma_i}$$

- $\mathbf{m} \in \mathcal{M}(\mathcal{X})^{\mathbf{2}}$ is a vector Radon measure;
- $\mathscr{V} \overset{\text{def.}}{=} \{\mathbf{m} \in \mathcal{M}(\mathcal{X})^{\mathbf{2}}, \operatorname{div}(\mathbf{m}) \in \mathcal{M}(\mathcal{X})\}$

Curve reconstruction with CROC energy

CROC functional: [Laville, Blanc-Féraud, Aubert 2023]

$$\arg\min_{\mathbf{m}\in\mathscr{V}} \frac{1}{2}\|\mathbf{y}-\Psi\mathbf{m}\|_2^2 + \alpha(\|\mathbf{m}\|_{\mathsf{TV}^2} + \|\operatorname{div}\mathbf{m}\|_{\mathsf{TV}})$$

$$\mathbf{m}^* = \sum_{i=1}^{r} a_i \mu_{\gamma_i}$$

- $\mathbf{m} \in \mathcal{M}(\mathcal{X})^{\mathbf{2}}$ is a vector Radon measure;
- $\mathscr{V} \overset{\text{def.}}{=} \{\mathbf{m} \in \mathcal{M}(\mathcal{X})^{\mathbf{2}}, \operatorname{div}(\mathbf{m}) \in \mathcal{M}(\mathcal{X})\}$
- Result from the **representer theorem**: one of the minimizers is a finite sum of measures supported on curves μ_γ.

Curve reconstruction with CROC energy

CROC functional: [Laville, Blanc-Féraud, Aubert 2023]

$$\arg\min_{\mathbf{m}\in\mathscr{V}} \frac{1}{2}\|\mathbf{y}-\Psi\mathbf{m}\|_2^2 + \alpha(\|\mathbf{m}\|_{\mathsf{TV}^2} + \|\operatorname{div}\mathbf{m}\|_{\mathsf{TV}})$$

$$\mathbf{m}^* = \sum_{i=1}^{r} a_i \mu_{\gamma_i}$$

- $\mathbf{m} \in \mathcal{M}(\mathcal{X})^{\mathbf{2}}$ is a vector Radon measure;
- $\mathscr{V} \overset{\text{def.}}{=} \{\mathbf{m} \in \mathcal{M}(\mathcal{X})^{\mathbf{2}}, \operatorname{div}(\mathbf{m}) \in \mathcal{M}(\mathcal{X})\}$
- Result from the **representer theorem**: one of the minimizers is a finite sum of measures supported on curves μ_γ.
  Let $\gamma : [0,1] \to \mathbb{R}^2$ a 1-rectifiable parametrised Lipschitz curve, we say that $\mu_\gamma \in \mathscr{V}$ *is a measure* ***supported on a curve*** γ if:

$$\forall \varphi \in \boldsymbol{\mathcal{C}_0(\mathcal{X})^2}, \quad \langle \mu_\gamma, \varphi \rangle_{\boldsymbol{\mathcal{M}^2 \times \mathcal{C}_0(\mathcal{X})^2}} \overset{\text{def.}}{=} \int_0^1 \varphi(\gamma(t)) \cdot \dot{\gamma}(t)\, \mathrm{d}t.$$

Curve reconstruction with CROC energy

CROC functional: [Laville, Blanc-Féraud, Aubert 2023]

$$\arg\min_{\mathbf{m}\in\mathscr{V}} \frac{1}{2}\|\mathbf{y}-\Psi\mathbf{m}\|_2^2 + \alpha(\|\mathbf{m}\|_{\mathsf{TV}^2} + \|\operatorname{div}\mathbf{m}\|_{\mathsf{TV}})$$

$$\mathbf{m}^* = \sum_{i=1}^{r} a_i \mu_{\gamma_i}$$

- $\mathbf{m} \in \mathcal{M}(\mathcal{X})^{\mathbf{2}}$ is a vector Radon measure;
- $\mathscr{V} \overset{\text{def.}}{=} \{\mathbf{m} \in \mathcal{M}(\mathcal{X})^{\mathbf{2}}, \operatorname{div}(\mathbf{m}) \in \mathcal{M}(\mathcal{X})\}$
- Result from the **representer theorem**: one of the minimizers is a finite sum of measures supported on curves μ_γ.
  Let $\gamma : [0,1] \to \mathbb{R}^2$ a 1-rectifiable parametrised Lipschitz curve, we say that $\mu_\gamma \in \mathscr{V}$ *is a measure* ***supported on a curve*** γ if:

$$\forall \varphi \in \boldsymbol{\mathcal{C}_0(\mathcal{X})^2}, \quad \langle \mu_\gamma, \varphi \rangle_{\boldsymbol{\mathcal{M}^2 \times \mathcal{C}_0(\mathcal{X})^2}} \overset{\text{def.}}{=} \int_0^1 \varphi(\gamma(t)) \cdot \dot{\gamma}(t)\, \mathrm{d}t.$$

- $\|\mu_\gamma\|_{\mathsf{TV}^2} = \mathscr{H}_1(\gamma((0,1)))$ is the curve length ;

Curve reconstruction with CROC energy

CROC functional: [Laville, Blanc-Féraud, Aubert 2023]

$$\arg\min_{\mathbf{m}\in\mathscr{V}} \frac{1}{2}\|\mathbf{y}-\Psi\mathbf{m}\|_2^2 + \alpha(\|\mathbf{m}\|_{\mathsf{TV}^2} + \|\operatorname{div}\mathbf{m}\|_{\mathsf{TV}})$$

$$\mathbf{m}^* = \sum_{i=1}^{r} a_i \mu_{\gamma_i}$$

- $\mathbf{m} \in \mathcal{M}(\mathcal{X})^{\mathbf{2}}$ is a vector Radon measure;
- $\mathscr{V} \overset{\text{def.}}{=} \{\mathbf{m} \in \mathcal{M}(\mathcal{X})^{\mathbf{2}}, \operatorname{div}(\mathbf{m}) \in \mathcal{M}(\mathcal{X})\}$
- Result from the **representer theorem**: one of the minimizers is a finite sum of measures supported on curves μ_γ.
  Let $\gamma : [0,1] \to \mathbb{R}^2$ a 1-rectifiable parametrised Lipschitz curve, we say that $\mu_\gamma \in \mathscr{V}$ *is a measure* ***supported on a curve*** γ if:

$$\forall \varphi \in \boldsymbol{\mathcal{C}_0(\mathcal{X})^2}, \quad \langle \mu_\gamma, \varphi \rangle_{\boldsymbol{\mathcal{M}^2 \times \mathcal{C}_0(\mathcal{X})^2}} \overset{\text{def.}}{=} \int_0^1 \varphi(\gamma(t)) \cdot \dot{\gamma}(t)\, \mathrm{d}t.$$

- $\|\mu_\gamma\|_{\mathsf{TV}^2} = \mathscr{H}_1(\gamma((0,1)))$ is the curve length ;
- $\|\operatorname{div}\mu_\gamma\|_{\mathsf{TV}}$ is the (open) curve counting term.

Curve reconstruction with CROC energy

$$\arg\min_{\mathbf{m}\in\mathscr{V}} \frac{1}{2}\|\mathbf{y}-\Psi\mathbf{m}\|_2^2 + \alpha(\|\mathbf{m}\|_{\mathsf{TV}^2} + \|\mathrm{div}\,\mathbf{m}\|_{\mathsf{TV}})$$

$$\mathbf{m}^* = \sum_{i=1}^{r} a_i \mu_{\gamma_i}$$

- $\mathbf{m} \in \mathcal{M}(\mathcal{X})^{\mathbf{2}}$ is a vector Radon measure;
- $\mathscr{V} \overset{\text{def.}}{=} \{\mathbf{m} \in \mathcal{M}(\mathcal{X})^{\mathbf{2}}, \mathrm{div}(\mathbf{m}) \in \mathcal{M}(\mathcal{X})\}$

Curve reconstruction with CROC energy

$$\arg\min_{\mathbf{m}\in\mathscr{V}} \frac{1}{2}\|\mathbf{y}-\Psi\mathbf{m}\|_2^2 + \alpha(\|\mathbf{m}\|_{\mathsf{TV}^2} + \|\mathrm{div}\,\mathbf{m}\|_{\mathsf{TV}})$$

$$\mathbf{m}^* = \sum_{i=1}^{r} a_i \mu_{\gamma_i}$$

- $\mathbf{m} \in \mathcal{M}(\mathcal{X})^{\mathbf{2}}$ is a vector Radon measure;
- $\mathscr{V} \overset{\text{def.}}{=} \{\mathbf{m} \in \mathcal{M}(\mathcal{X})^{\mathbf{2}},\, \mathrm{div}(\mathbf{m}) \in \mathcal{M}(\mathcal{X})\}$

- **Smirnov decomposition into curves** [Smirnov 1994; Rodríguez & Wengenroth 2024; Irving 2025]

$$\forall \mathbf{m} \in \mathcal{V}(\mathcal{X}), \exists\, \nu \in \mathcal{M}^+(\mathcal{K}^{\mathsf{Smirv}}),$$

$$\boxed{\mathbf{m} = \int_{\mathcal{K}^{\mathsf{Smirv}}} \mu_\gamma \,\mathrm{d}\nu(\gamma), \quad |\mathbf{m}| = \int_{\mathcal{K}^{\mathsf{Smirv}}} |\mu_\gamma| \,\mathrm{d}\nu(\gamma)}$$

$$\boxed{\mathcal{K}^{\mathsf{Smirv}} = \left\{\gamma : [0,1] \to \mathbb{R}^2 \,\middle|\, \gamma \text{ is Lipschitz, } |\dot\gamma(t)| \leq 1 \text{ a.e.}\right\}}$$

where $|\mathbf{m}|$ is the Total Variation measure defined by

$$\forall A \in \mathcal{B}(\mathcal{X}), \quad |\mathbf{m}|(A) = \sup\left\{\langle \mathbf{m}, \varphi\rangle : \varphi \in \mathrm{C}_0(A, \mathbb{R}^2),\ \|\varphi\|_\infty \leq 1\right\}.$$

Curve reconstruction with CROC energy

CROC functional: [Laville, Blanc-Féraud, Aubert 2023]

$$\arg\min_{\mathbf{m}\in\mathcal{Y}} \frac{1}{2}\|\mathbf{y}-\Psi\mathbf{m}\|_2^2 + \alpha(\|\mathbf{m}\|_{\mathsf{TV}^2} + \|\operatorname{div}\mathbf{m}\|_{\mathsf{TV}})$$

$$\mathbf{m}^* = \sum_{i=1}^{r} a_i \mu_{\gamma_i}$$

Difficulties

- Define the observation term as $\mathbf{y}$ is intensity (scalar) and $\mathbf{m}$ is vectorial measure
- The term which gives numerical correct result is $\frac{1}{2}\|y - |\mathbf{m}| * h\|_2^2$
- No proof of existence of a solution, no representer theorem result.

Curve reconstruction with CLASSO energy

$$\underset{\sigma \in \mathcal{M}^+(S)}{\arg\min} \frac{1}{2}\|\mathbf{y} - \int_S (|\mu_\gamma| * h)\, \mathrm{d}\sigma(\gamma)\|_2^2 + \lambda \|\sigma\|_{\mathsf{TV}}$$

$$\sigma^* = \sum_{i=1}^{r} a_i \delta_{\gamma_i}$$

- **Smirnov decomposition into curves** [Smirnov 1994; Rodríguez & Wengenroth 2024; Irving 2025]

$\forall \mathbf{m} \in \mathcal{V}(\mathcal{X}), \exists\, \nu \in \mathcal{M}^+(\mathcal{K}^{\mathsf{Smirv}}),$

$$\mathbf{m} = \int_{\mathcal{K}^{\mathsf{Smirv}}} \mu_\gamma \, \mathrm{d}\nu(\gamma), \quad |\mathbf{m}| = \int_{\mathcal{K}^{\mathsf{Smirv}}} |\mu_\gamma| \, \mathrm{d}\nu(\gamma)$$

$$\mathcal{K}^{\mathsf{Smirv}} = \left\{ \gamma : [0,1] \to \mathbb{R}^2 \,\middle|\, \gamma \text{ is Lipschitz, } |\dot{\gamma}(t)| \leq 1 \text{ a.e.} \right\}$$

- Use Smirnov decomposition on S simple curves of $\mathcal{K}^{\mathsf{Smirv}}$ (plus some other technical constraints)
- **Representer theorem** with TV norm.

Curve reconstruction with CLASSO energy

$$\arg\min_{\sigma \in \mathcal{M}^+(S)} \frac{1}{2}\|\mathbf{y} - \int_S (|\mu_\gamma| * h)\, \mathrm{d}\sigma(\gamma)\|_2^2 + \lambda \|\sigma\|_{\mathsf{TV}}$$

$$\sigma^* = \sum_{i=1}^{r} a_i \delta_{\gamma_i}$$

$$J(\sigma^* = \sum_{i=1}^{r} a_i \delta_{\gamma_i}) = \frac{1}{2} \left\| \mathbf{y} - \Psi \left(\sum_{i=1}^{r} a_i \delta_{\gamma_i} \right) \right\|_2^2 + \lambda \sum_{i=1}^{r} a_i$$

Sliding Franck-Wolf Algorithm for curves

$$J(\sigma^* = \sum_{i=1}^{r} a_i \delta_{\gamma_i}) = \frac{1}{2} \left\| \mathbf{y} - \Psi \left(\sum_{i=1}^{r} a_i \delta_{\gamma_i} \right) \right\|_2^2 + \lambda \sum_{i=1}^{r} a_i$$

Initialize $k = 0$ and $\sigma^0 = 0$

Sliding Franck-Wolf Algorithm for curves

$$J(\sigma^* = \sum_{i=1}^{r} a_i \delta_{\gamma_i}) = \frac{1}{2} \left\| \mathbf{y} - \Psi \left(\sum_{i=1}^{r} a_i \delta_{\gamma_i} \right) \right\|_2^2 + \lambda \sum_{i=1}^{r} a_i$$

Initialize $k = 0$ and $\sigma^0 = 0$

- Compute the certificate $\eta^{[k]} = \frac{1}{\lambda} \Psi^*(\mathbf{y} - \Psi(\sigma^{[k]}))$
- Find a new atom $\gamma_*^{[k]}$ [LBFGS algorithm]

$$\gamma_*^{[k]} \in \arg\max_{\gamma \in S} \eta^{[k]}(\gamma).$$

- If $\eta^{[k]}(\gamma_*^{[k]}) \leq 1$, Then $\sigma^{[k]}$ is a solution [STOP]
- Else
  - add $\gamma_*^{[k]}$ to $\sigma^{[k]} = \sum_{i=1}^{k-1} a_i \delta_{\gamma_i} + a_k \delta_{\gamma_k}$
  - compute the optimal weights a_i by minimizing $J(\sigma^{[k]})$ [LBFGS algorithm]
  - Sliding step compute the optimal (a_i, γ_i) by minimizing $J(\sigma^{[k]})$ [ADAM algorithm]
  - Prune atome with negligible weights

Simulation results

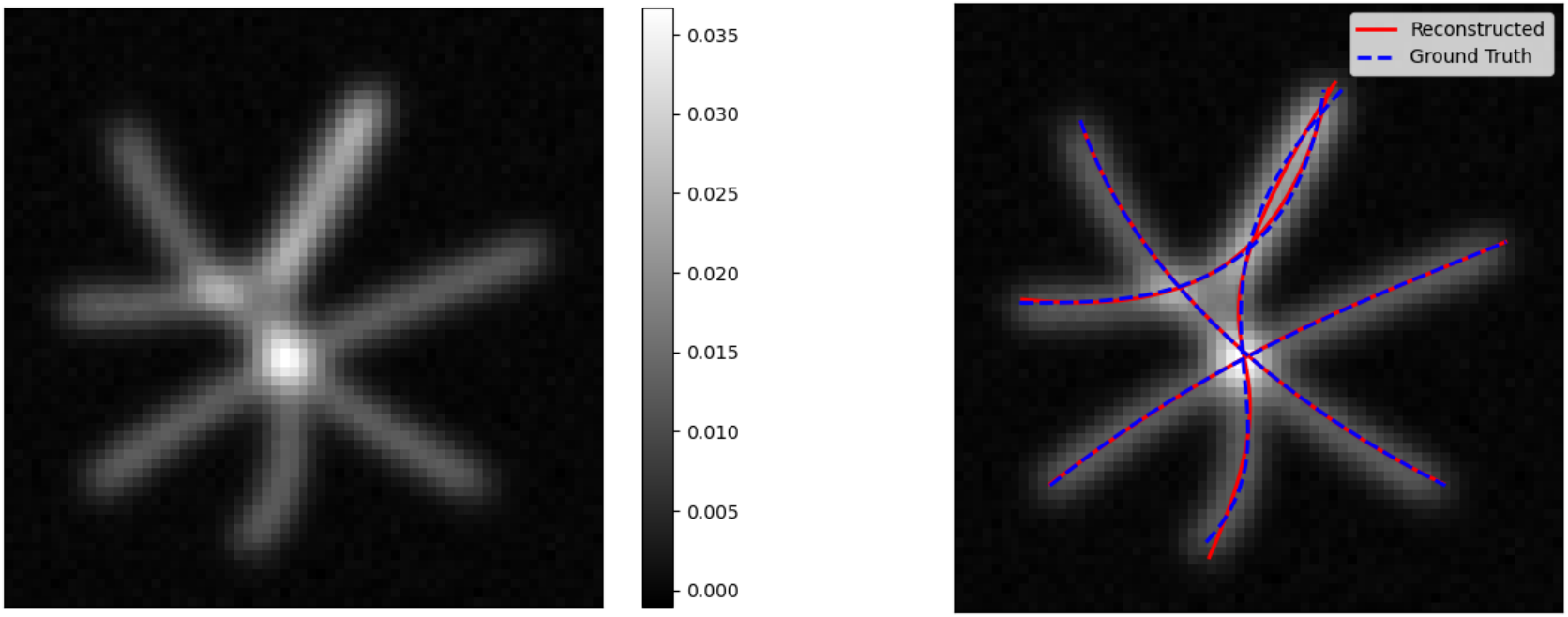

Figure: Illustrative results of curve reconstruction using the CLASSO framework. Left: input blurry and noisy image; right: curve reconstruction (red = reconstruction, blue = ground-truth). Curves are parametrized with 4 Bezier parameters.

Simulation results

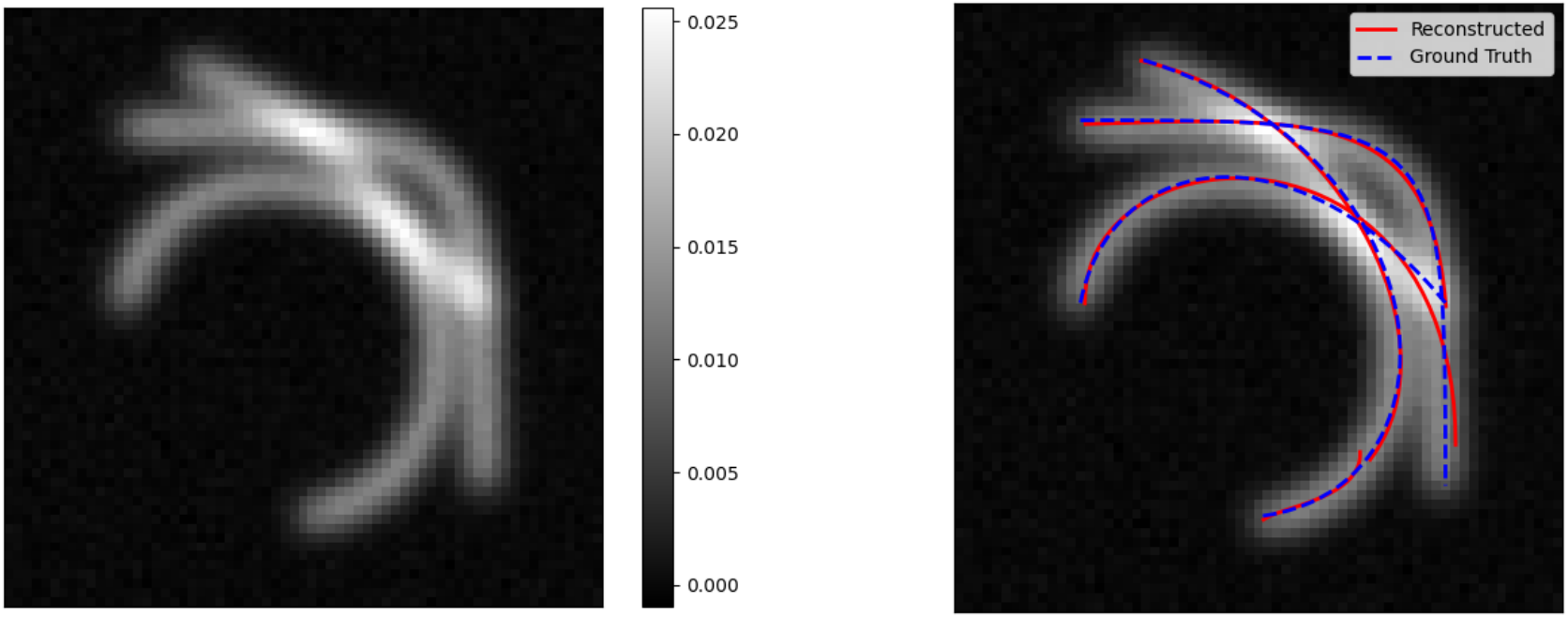

Figure: Illustrative results of curve reconstruction using the CLASSO framework. Left: input blurry and noisy image; right: curve reconstruction (red = reconstruction, blue = ground-truth).

Off-the-grid method for curves


B. Laville, L. Blanc-Féraud, G. Aubert *Siam Journal of Imaging Sciences*, 2023.


A. Tsafack, L. Blanc-Féraud, G. Aubert *ESAIM: Control, Optimisation and Calculus of Variations*, submitted.

Code available at `https://gitlab.inria.fr/blaville/amg`

Code available at `https://gitlab.inria.fr/atsafack/implementation_of_the_sfw_algorithm_for_the_classo_functional`

Continuing on curves

- Discretisation of the curves (splines, Bezier)
- Avoid discretisation of the curve with Neural fields
- Biological filaments with more complex configuration (varying intensity, fluorescent microscopy images...)
- Super-resolution by fluctuations
- Extension to spatial (3D) super-resolution (e.g. combining with MA-TIRF or bi-plan microscope).

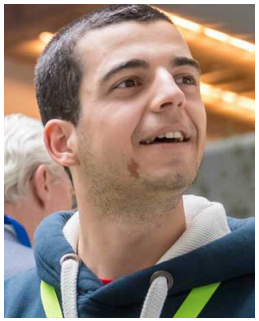
Mayeul Cachia


Vasilina Stergiopoulou


Bastien Laville


Aneva Tsafack

Thank you for your attention


Gilles Aubert


Luca Calatroni


Sébastien Schaub

Super-Resolution: Fluctuation-based Methods

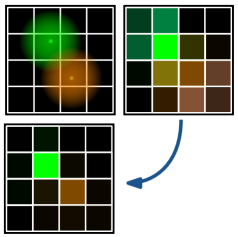

SOFI [Dertinger *et al.*, '09]
Super resolution Optical Fluctuation Imaging

- Shrinkage of PSF via computation of higher-order statistics

SRRF [Gustafsson *et al.*, '16]
Super-Resolution Radial Fluctuations

- Non-linear transformation of frames based on radial symmetry

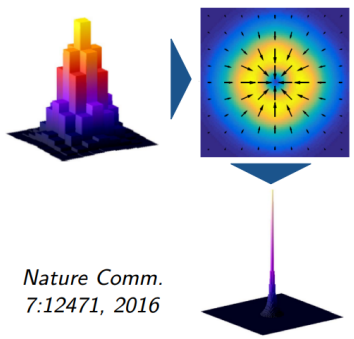

Nature Comm. 7:12471, 2016

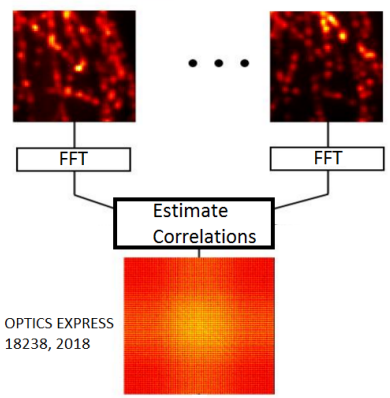

SPARCOM [Solomon *et al.*, '19], **COLORME** [Stergiopoulou *et al.*, '22],
SPARsity based super-resolution COrrelation Microscopy

- Exploits sparsity in the correlation domain

Standard approach: COLORME summary

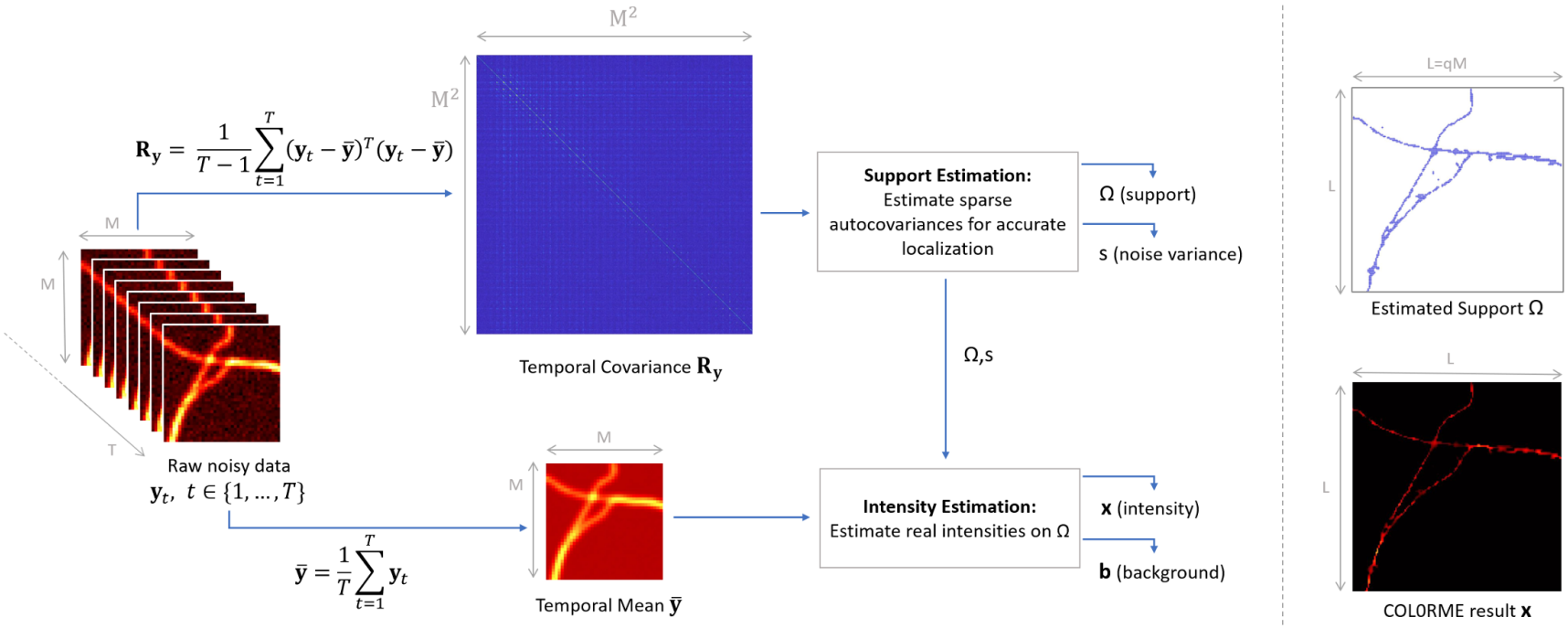

Standard approach: COLORME summary

$$\underset{\mathbf{r_x}\geq 0, s\geq 0}{\arg\min} \ \frac{1}{2}\|\mathbf{r_y} - (\mathbf{\Psi}\odot\mathbf{\Psi})\mathbf{r_x} - s\mathbf{I_v}\|_2^2 + \lambda R(\mathbf{r_x})$$

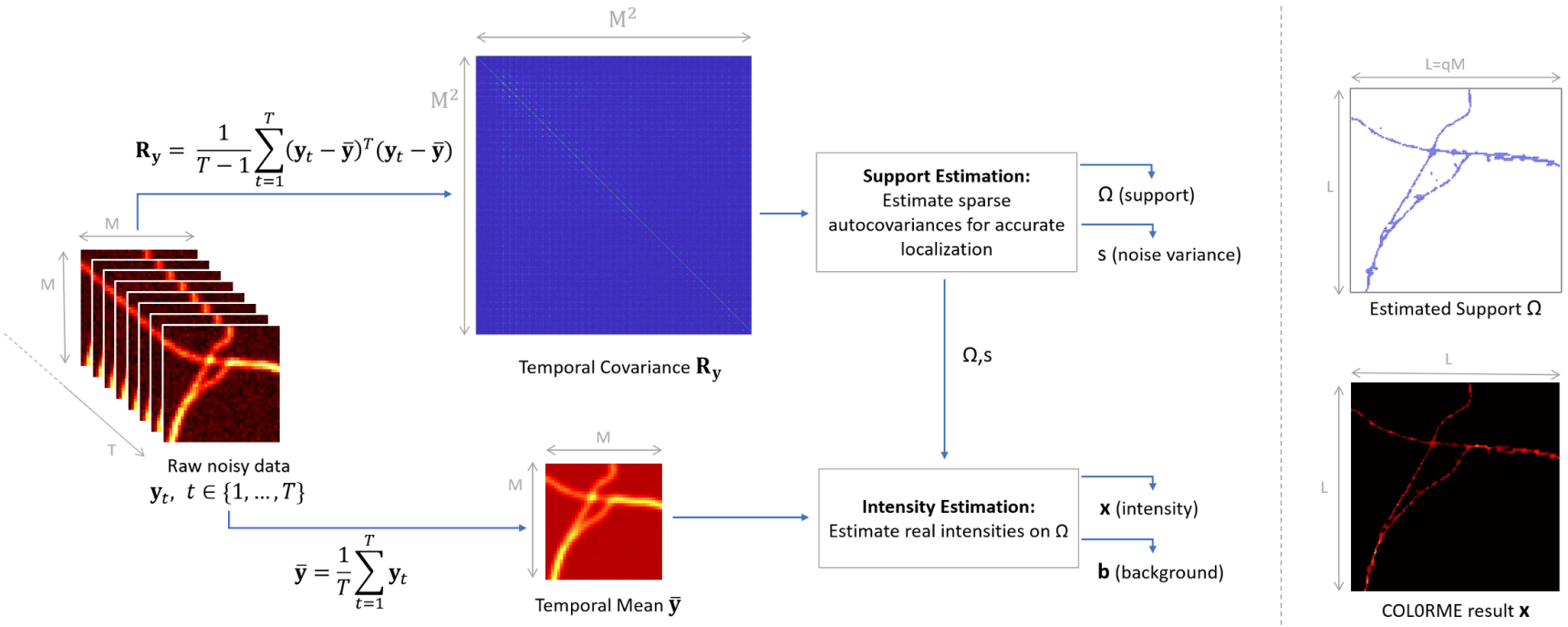

$$\underset{\mathbf{x}\in\mathbb{R}^{|\Omega|},\ \mathbf{b}\in\mathbb{R}^{M^2}}{\arg\min} \ \frac{1}{2}\|\bar{\mathbf{y}} - \mathbf{\Psi_\Omega}\mathbf{x} - \mathbf{b}\|_2^2 + \mu\|\nabla\mathbf{x}\|_2^2 + \beta\|\nabla\mathbf{b}\|_2^2 + \iota_{\geq 0}(\mathbf{x}) + \iota_{\geq 0}(\mathbf{b})$$

Optimisation insights

- Computation of $\frac{\partial}{\partial \mathbf{x}} \mathbf{y}_m^{\text{sim}}(\mathbf{x}, \mathbf{b})$ tricky due to the dependence on Poisson process $\mathbf{y}_m^{\text{sim}} = \mathcal{P}(\mathbf{\Psi} \mathbf{x}_m + \mathbf{b}) + \mathbf{n}_m$. Approximation and use of techniques from stochastic computation graphs [1].
- Explicit computation of $\nabla_{\mathbf{x}}$, $\nabla_{\mathbf{b}}$ for model-driven regularisation terms
- Architecture of $D_{\varphi} \in [0, 1]$ inspired by CryoGAN

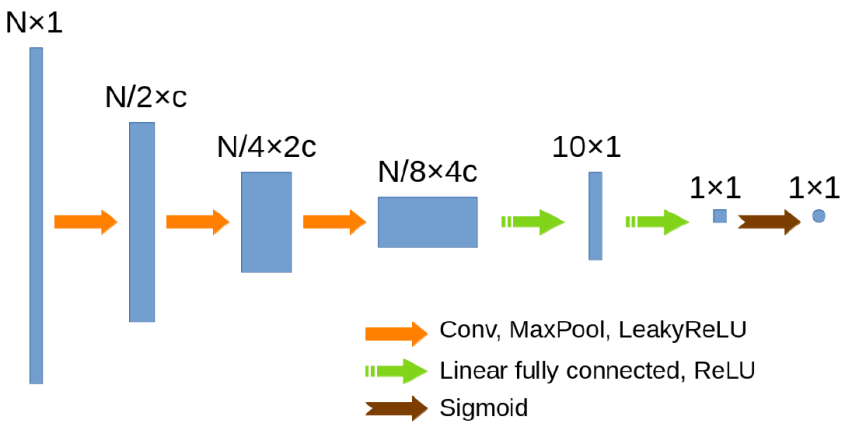

- `Pytorch` backpropagation for $\nabla_{\varphi} D_{\varphi}(\cdot)$
- ADAM/stochastic proximal algorithms for optimisation

[1] [Schulman, Heess, Weber, Abbeel, '15]

Reconstruction of sets

BV functional: [Rudin, Osher, Fatemi 1992; Petit, Duval, Peyré 2022]

$$\arg\min_{u \in \mathrm{BV}(\mathcal{X})} \frac{1}{2}\|\mathbf{y} - \Psi u\|_2^2 + \lambda \|u\|_{BV}$$

$$u^* = \sum_{i=1}^{N} a_i \chi_{E_i}$$

- $\mathrm{BV}(\mathcal{X}) = \left\{ u \in \mathrm{L}^1(\mathcal{X}) \mid \mathrm{D}u \in \mathcal{M}(\mathcal{X})^{\mathbf{2}} \right\}$
  $\|u\|_{BV} \overset{\text{def.}}{=} \|u\|_1 + \|\mathrm{D}u\|_{\mathbf{TV}^2}.$

Reconstruction of sets

BV functional: [Rudin, Osher, Fatemi 1992; Petit, Duval, Peyré 2022]

$$\arg\min_{u \in \mathrm{BV}(\mathcal{X})} \frac{1}{2}\|\mathbf{y} - \Psi u\|_2^2 + \lambda \|u\|_{BV} \qquad u^* = \sum_{i=1}^{N} a_i \chi_{E_i}$$

- $\mathrm{BV}(\mathcal{X}) = \left\{ u \in \mathrm{L}^1(\mathcal{X}) \mid \mathrm{D}u \in \mathcal{M}(\mathcal{X})^{\mathbf{2}} \right\}$
  $\|u\|_{BV} \overset{\text{def.}}{=} \|u\|_1 + \|\mathrm{D}u\|_{\mathbf{TV}^2}.$

- Result from the **representer theorem**: one of the minimizers is a finite sum of indicator functions of sets.

Reconstruction of sets

BV functional: [Rudin, Osher, Fatemi 1992; Petit, Duval, Peyré 2022]

$$\arg\min_{u \in \mathrm{BV}(\mathcal{X})} \frac{1}{2}\|\mathbf{y} - \Psi u\|_2^2 + \lambda \|u\|_{BV} \qquad u^* = \sum_{i=1}^{N} a_i \chi_{E_i}$$

- $\mathrm{BV}(\mathcal{X}) = \left\{ u \in \mathrm{L}^1(\mathcal{X}) \mid \mathrm{D}u \in \mathcal{M}(\mathcal{X})^{\mathbf{2}} \right\}$
  $\|u\|_{BV} \overset{\text{def.}}{=} \|u\|_1 + \|\mathrm{D}u\|_{\mathsf{TV}^2}$.
- Result from the **representer theorem**: one of the minimizers is a finite sum of indicator functions of sets.
- If $u = \chi_E$, indicator function of a simple set $E \subset \mathcal{X}$, $\|\mathrm{D}u\|_{\mathsf{TV}^2} = \mathrm{Per}(E)$

Geometry encoded in off-the-grid

	TV	BV
Geometry	Spikes	Sets
Space	$\mathcal{M}(\mathcal{X})$	$\mathrm{BV}(\mathcal{X})$
Regulariser	$\|\cdot\|_{\mathrm{TV}}$	$\|\cdot\|_1 + \|\mathrm{D}\cdot\|_{\mathrm{TV}^2}$

δ_x

Geometry encoded in off-the-grid

	TV	BV
Geometry	Spikes	Sets
Space	$\mathcal{M}(\mathcal{X})$	$\mathrm{BV}(\mathcal{X})$
Regulariser	$\|\cdot\|_{\mathrm{TV}}$	$\|\cdot\|_1 + \|\mathrm{D}\cdot\|_{\mathrm{TV}^2}$

δ_x

χ_E

Geometry encoded in off-the-grid

	TV	?	BV
Geometry	Spikes	Curves	Sets
Space	$\mathcal{M}(\mathcal{X})$	?	$\mathrm{BV}(\mathcal{X})$
Regulariser	$\|\cdot\|_{\mathrm{TV}}$	?	$\|\cdot\|_1 + \|\mathrm{D}\cdot\|_{\mathrm{TV}^2}$

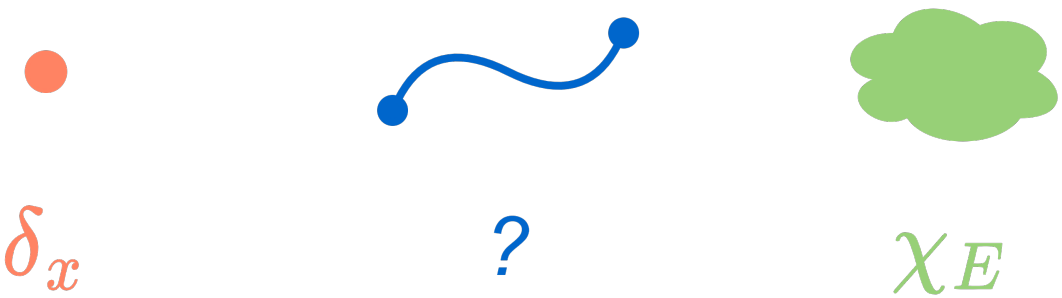

δ_x ? χ_E

A new functional space for curves

- let $\mathcal{M}(\mathcal{X})^{\mathbf{2}}$ be the space of vector Radon measures;
- let $\mathscr{Y} \overset{\text{def.}}{=} \left\{\mathbf{m} \in \mathcal{M}(\mathcal{X})^{\mathbf{2}}, \operatorname{div}(\mathbf{m}) \in \mathcal{M}(\mathcal{X})\right\}$ the space of *charges*, or *divergence vector fields*. It is a Banach equipped with $\|\cdot\|_{\mathscr{Y}} \overset{\text{def.}}{=} \|\cdot\|_{\mathsf{TV}^2} + \|\operatorname{div}(\cdot)\|_{\mathsf{TV}}$;

- let $\gamma : [0,1] \to \mathbb{R}^d$ a 1-rectifiable parametrised Lipschitz curve,

A new functional space for curves

- let $\mathcal{M}(\mathcal{X})^{\mathbf{2}}$ be the space of vector Radon measures;
- let $\mathscr{V} \overset{\text{def.}}{=} \left\{\mathbf{m} \in \mathcal{M}(\mathcal{X})^{\mathbf{2}}, \operatorname{div}(\mathbf{m}) \in \mathcal{M}(\mathcal{X})\right\}$ the space of *charges*, or *divergence vector fields*. It is a Banach equipped with $\|\cdot\|_{\mathscr{V}} \overset{\text{def.}}{=} \|\cdot\|_{\mathsf{TV}^2} + \|\operatorname{div}(\cdot)\|_{\mathsf{TV}}$;

- let $\gamma : [0,1] \to \mathbb{R}^d$ a 1-rectifiable parametrised Lipschitz curve, we say that $\mu_\gamma \in \mathscr{V}$ *is a measure* ***supported on a curve*** γ if:

$$\forall \mathbf{g} \in \boldsymbol{\mathcal{C}_0(\mathcal{X})^{\mathbf{2}}}, \quad \langle \mu_\gamma, \mathbf{g} \rangle_{\boldsymbol{\mathcal{M}^{\mathbf{2}} \times \mathcal{C}_0(\mathcal{X})^{\mathbf{2}}}} \overset{\text{def.}}{=} \int_0^1 \mathbf{g}(\gamma(t)) \cdot \dot{\gamma}(t) \, \mathrm{d}t.$$

- a curve is closed is $\gamma(0) = \gamma(1)$, open otherwise;
- simple if γ is an injective mapping
- $\|\mu_\gamma\|_{\mathsf{TV}^2} = \mathscr{H}_1(\gamma((0,1)))$, curve length
- $\operatorname{div} \mu_\gamma = \delta_{\gamma(0)} - \delta_{\gamma(1)}$, counts the number of open curves.

Extreme points

Definition

Let X be a topological vector space and $K \subset X$ convex. An *extreme point* x of K is a point such that $\forall y, z \in K$:

$$\forall \lambda \in (0,1),\ x = \lambda y + (1-\lambda) z \implies x = y = z$$

$\operatorname{Ext} K$ is the set of extreme points of K.

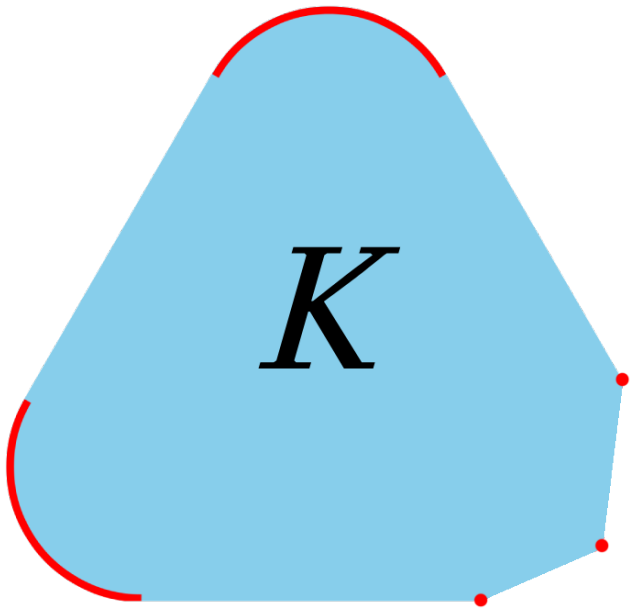

$\operatorname{Ext} K$ in red

Representer theorem

Let $F : Z \to \mathbb{R}$, G the data-term, R the regulariser, $\lambda > 0$.

$$F = G + \lambda R$$

Theorem (Representer theorem)

Under some hypothesis on F, there exists a minimiser of F which is a **linear finite sum** *of extreme points of the unit-ball of R, $\operatorname{Ext} \mathcal{B}_R^1 \overset{\text{def.}}{=} \{u \in Z \,|\, R(u) \leq 1\}$.*

[Bredies & Carioni 2019, Boyer et al. 2019]

Characterise $\operatorname{Ext} \mathcal{B}_R^1$ of the regulariser $\iff$ outline the structure of a *minimum* of F.

CLASSO

$$\mathcal{K} = \left\{ \gamma \in C^3([0,1];\mathbb{R}^2) \;\middle|\; \|\dot{\gamma}\| \leq 1,\ \|\ddot{\gamma}\| \leq 2\sqrt{2},\ \|\gamma^{(3)}\| \leq L,\ \|\gamma^{(4)}(t)\| \leq M \text{ a.e.} \right\}$$

Simulations results

$$J(\sigma^* = \sum_{i=1}^{N} a_i \delta_{\gamma_i}) = \frac{1}{2} \left\| y - \Psi \left(\sum_{i=1}^{N} a_i \delta_{\gamma_i} \right) \right\|_2^2 + \lambda \sum_{i=1}^{N} a_i$$

- We use cubic Bezier parametrized curves for γ_i.
- Optimization of the certificat is obtain with L-BFGS algorithm initialized the curve obtained by
  - compute the absolute value of the certificate $\eta^{[k]}$
  - Threshold to extract a skeleton
  - Find 4 points of curve along this skeleton, included 2 endpoints.
  - Initialize the 4 Bezier parameters with these 4 points.